TALLINNA TEHNIKAÜLIKOOL
INSENERITEADUSKOND

Elektroenergeetika ja mehhatroonika instituut

TSENTRIFUGAALPUMBA VÕIMSUSE HALDAMINE MUUDETAVA KIIRUSEGA AJAMI ABIL

POWER MANAGEMENT OF A CENTRIFUGAL PUMP WITH A VARIABLE-SPEED DRIVE

MAGISTRITÖÖ

Üliõpilane:	Aleksandr Serbin
Üliõpilaskood:	132147AAAM
Juhendaja:	Professor Valery Vodovozov

Tallinn, 2017.a.

AUTORIDEKLARATSIOON

Olen koostanud lõputöö iseseisvalt.
Lõputöö alusel ei ole varem kutse- või teaduskraadi või inseneridiplomit taotletud. Kõik töö koostamisel kasutatud teiste autorite tööd, olulised seisukohad, kirjandusallikatest ja mujalt pärinevad andmed on viidatud.

"......." .... 201…..

Autor: ....
            / allkiri /

Töö vastab bakalaureusetöö/magistritööle esitatud nõuetele

"......." .... 201…..

Juhendaja: ....
            / allkiri /

Kaitsmisele lubatud

"......."....................201… .

Kaitsmiskomisjoni esimees ....
                            / nimi ja allkiri /

Referaat:

Antud töö eesmärk on välja töötada praktilise meetodi tsentrifugaalpumba töö optimaalpunkti leidmiseks, milles kogu süsteemi võimsus on minimaalne.

Peale selle töös on käsitletud pumbade töösuutlikkus väljaspoole tootjaga kindlaksmääratud valdkondadele, mis on aga paljude pumbade igapäevast tööst osa.

Autor on välja töötatud ja testitud mitmeid programme. Esimene neist on ettenähtud ajamist, tsentrifugaal pumbast ja juhitavast drosselist koosnevast süsteemi õpetamiseks. Teised programmid kasutavad andmed, mis olid saadud süsteemi õpetamise protsessis, kõige optimaalsema töörežiimi leidmiseks ja pumba ajamite juhtimiseks.

On välja töötatud 3 optimeerimise meetodit: otsimine tabelimeetodiga, otsimine tabeli-analüütimise meetodiga nurgapunktide läbi ja otsimine tabeli-analüütimise meetodiga kõiki punkte arvesse võttes.

Kõik meetodid nii optimaalpunkti otsimiseks, kui ka süsteemi õpetamiseks oli testitud reaalses süsteemis.

Eksperimendi tulemused on lõputöös esitatud.

ATV70LT

Управление мощностью центробежного насоса с помощью частотно-регулируемого привода

Александр Сербин, код студента 132147АААМ, май 2017. – 64 стр.

ТАЛЛИНСКИЙ ТЕХНИЧЕСКИЙ УНИВЕРСИТЕТ * Инженерный факультет

Институт электроэнергетики и мехатроники

Кафедра электропривода и электроснабжения

Руководитель работы: профессор Валерий Водовозов

Реферат:

Целью данной работы является разработка практического метода нахождения оптимальной точки работы центробежного насоса, в которой потребляемая мощность всей системы будет минимальна.

Помимо этого рассматривается возможность функционирования насосов за пределами областей, рекомендуемых производителями, но являющихся частью повседневной работы многих насосов.

Автором разработаны и испытаны несколько программ. Первая из них предназначена для обучения системы, состоящей из электроприводов, центробежного насоса и управляемого дросселя. Другие программы используют полученные в результате обучения системы данные, для поиска наиболее оптимального режима работы и управления приводами насосной установки.

Разработаны три метода оптимизации: поиск табличным методом, поиск таблично-аналитическим методом через угловые точки и поиск таблично-аналитическим методом с учётом всех точек.

Все предложенные методы обучения и оптимального управления прошли тестирование в реальной системе. Экспериментальные результаты представлены в дипломной работе.

Abstract:

The purpose of this research is to develop a practical method for finding an optimal mode of a centrifugal pump operation, at which power consumption of entire system will be minimal.

Besides, pump operation ability is considered outside the areas recommended by manufacturers that represent a part of regular performance for many pumping plants.

Several programs were developed by the author. The first one is intended for learning a system consisting of electrical drives, centrifugal pump, and controlled throttle. Other programs use the data obtained from system learning to search an optimal operation mode and to provide the pumping plant performance.

Three optimization methods are developed in the thesis: the search using the tabularized method, the search using the combined tabularized-analytical method with corner points, and the search using the combined method taking into account all the points.

All the proposed methods of system learning and optimal power management were validated in real pumping plant. Experimental results are presented in the thesis.

TABLE OF CONTENTS

KOOSKÕLASTATUD

Prof. Ivo Palu..............................

.... 2017

MAGISTRITÖÖ ÜLESANNE

Aleksandr Serbin, üliõpilaskood 132147AAAM

Magistritöö teema: Tsentrifugaalpumba võimsuse haldamine muudetava kiirusega ajami abil

Ülesanne: Välja töötada praktilise meetodi tsentrifugaalpumba töö optimaalpunkti leidmiseks, milles kogu süsteemi võimsus on minimaalne.

Lähteandmed:
1. Teststand tsentrifugaalpumbaga
2. Pumba spetsifikatsioon
3. ACQ810 kasutusejuhend
4. Koondplaan
5. Eelmist töö tulemused

Lahendamisele kuuluvate probleemide loetelu:
Leida tsentrifugaalpumba töö optimaalpunkti, milles kogu süsteemi võimsus on minimaalne:
1. Õpetada tsentrifugaalpumba süsteemi.
2. Valmistada optimeerimise taablimeetodiga.
3. Valmistada optimeerimise tabeli-analüütimise meetodiga nurgapunktide läbi.
4. Valmistada optimeerimise tabeli-analüütimise meetodiga kõiki punkte arvesse võttes.
5. Testida kõik meetodid teststandil.

Juhendaja: Ülesande vastu võtnud:

Professor V. Vodovozov ....   Üliõpilane A. Serbin ....

1. FOREWORD

This master's degree thesis was written by the author during his work in ABB Estonia and in Department of Electrical Power Engineering and Mechatronics of Tallinn University of Technology.

I would like to express my appreciation and gratitude to my supervisor Professor Valery Vodovozov and my fellow colleagues PhD Ilja Bakman and PhD student Levon Gevorkov for their kind attitude and help.

2. INTRODUCTION

2.1 Motivation

Centrifugal pumping stations are applied worldwide for liquid distribution, providing up to 90% of full water treatment. Among all the electricity consumers, pumping systems account for nearly 20 % of world energy and produce above 80 million tones of emissions [1] [2]. This is the reason for the need to develop more and more effective ways of pump regulation. Despite the fact that over the last century many improvements have been offered by the scientific community, the overall efficiency of pumping systems is still at a fairly low level, about 30 to 40% [3]. If the pump is forced to work in regions other than those recommended by manufacturers, the overall efficiency will be even lower. Poor efficiency can translate into other problems in hydraulic systems. Along with the growth of power consumption exhaust emissions (in the case of internal combustion engines) and operating costs increase also leading to the necessity of installing larger pumps and elaborate more cooling equipment to dissipate the heat. [4]

To meet energy saving and emission decrease requirements, all the interacting system resources – pumps, VSDs, control equipment, and network infrastructure – are to be discussed together.

2.2 Current problems

This is good if the pump has the possibility to operate in nominal area. However, the pump operation area may vary depending on needs of user. As soon as the demand for pressure or flow changes, the pump is no longer able to work in a nominal area. The problem can be solved by purchasing a new pumping system designed to work in that region, but the user often does not have the desire to do so for the financial or other reasons.

As the nominal areas of pumps, their drives, and gears have usually different locations, operating within one of them can cause mechanical deflections, hydraulic instability, or additional electrical losses for other parts.

The number of factors affecting the efficiency of the pump system is too great for the possibility of finding a solution analytically. Even with the full covered system, the collected data will

become obsolete in case of condition change. In addition, it is very complicated to associate the pump speed and the throttle angle with the system's determined state.

2.3 Targets and tasks

The targets of this research is to develop a practical method for finding an optimal mode of a centrifugal pump operation, at which power consumption of entire system will be minimal.

From the objective described above, the following research tasks were stated:

1. Analysis of the power management problems of centrifugal pumping plants and problem statement.
2. Preparation of a methodology for automatic estimation of the system characteristics under different system and pumping conditions.
3. Development of an algorithm for system learning.
4. Development of algorithms for finding the optimal operation modes using the data collected during the system learning.
5. Development of the pumping management procedures using the designed algorithms.
6. Validation of developed algorithms and management procedures in a real pumping system.

3. CENTRIFUGAL PUMPING PLANTS

Centrifugal pumps are widely used in everyday life in water supply networks, sewerage systems, oil production, and many other industries where they are used to transport liquids by the conversion of rotational kinetic energy of an electrical motor to the hydrodynamic energy of the liquid flow. One of the most attractive features of centrifugal pumps is their ability to perform under a broad range of operating conditions. They operate satisfactorily with different liquid types, densities, varying properties, at multiple loads and velocities.

A simplified diagram of a typical centrifugal pump in Fig. 3.1 shows relative locations of the pump parts [5] [6]. It consists of a stationary casing and an impeller mounted on a rotating shaft. Liquid enters via the suction (inlet) axially through eye of the casing being caught up in the impeller blades that impart its radial and rotary motion. Then, it is whirled tangentially and radially outward coming to the outer periphery called a volute. The fluid gains both velocity and pressure and finally leaves the pump through the discharge (outlet).
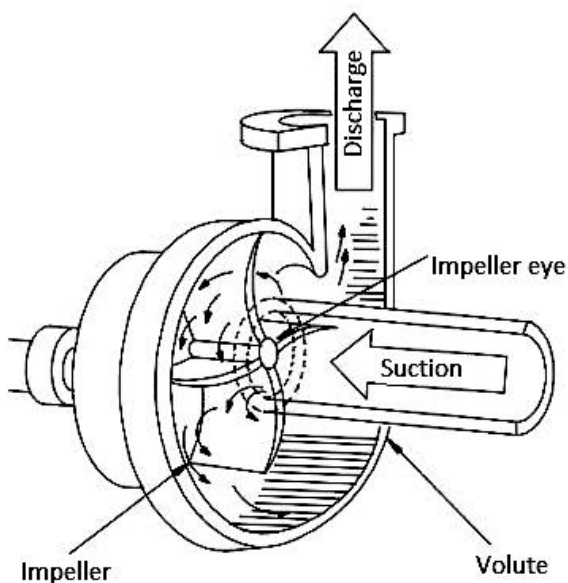
Fig. 3.1. Centrifugal pump.

Centrifugal pumping plants dominate in a variety of infrastructure systems, such as artificial waterways, shipping, and oil supply to consumers, the drainage of low-lying lands, and the sewage removal from processing sites. The centrifugal pumping plant represent facilities that involve both the pumps and accompanying equipment for pumping liquids from one place to another, such as piping, pipeline networks, tanks, and appropriate inline components: fittings,

valves, and devices that typically sense and control the flowrate, pressure, and temperature of the transmitted liquids.

To rotate the pumps, electrical drives are used. Mostly, non-adjustable drives prevail. In this case, the liquid regulation is conducted with the help of discharge throttle. The variable-speed drives (VSD) bring substantial benefits to the pumping management. The speed control can be brought by the induction motor VSDs, synchronous machine VSDs, switch-reluctance motor drives, or some other drive systems. To increase control possibilities, programmable logical controllers PLCs are introduced to the contemporary pumping plants.

3.1 Pipeline properties and system characteristics

Total energy the pump must supply involves two components: a flowrate and a total head.

The amount of liquid displaced per unit time is called a flowrate [7] and designated as q in this work. The flowrate determines the pump capacity in overcoming the losses caused by liquid flow in the pipes, valves, bends, and other piping plant devices. These losses are completely flow-dependent and nonlinear. Hence, the flowrate represents the kinetic energy component of the pump output.

In general, losses are represented by the liquid head designated as h, which may be of two types: the static head and the friction head. The first one is simply the difference in height of the supply and destination tanks. It provides elevation energy lifted on a certain height. The static head is independent of flow.

The friction head, called also a dynamic head loss, is the loss to environment due to the movement of liquid through pipes and fittings in the system. It provides velocity energy that the moving objects have. This loss is proportional to the square of the flowrate.

The sum of the static and friction heads, called a total head, represents the amount of energy per unit weight of liquid the pump creates between its inlet and the outlet. The total head is expressed as a height of liquid surface above or below some reference level (usually the centerline of the pump).

A system characteristic $h_s(q)$, demonstrates how the total head varies with the flowrate. It may be represented as a set of points $\{[h_{si}q_{si}] \dots [h_{sj}q_{sj}]\}$ or as a polynomial:

$$h_s(q) = h_{S0} + C_S \cdot q^2,$$ (3.1.1)

where h_{S0} – system static head [m],

C_S – system friction (dynamic) factor,

S – designates a system state.

Its graphed representation exemplified in Fig. 3.1.1 is called a resistance curve or a system curve.
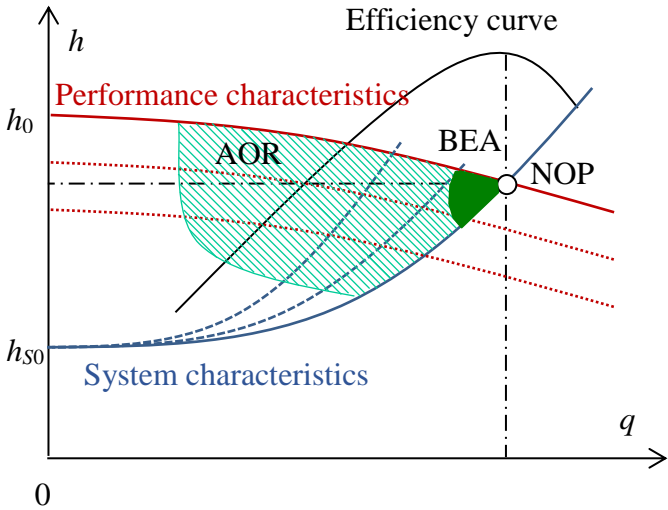
Fig. 3.1.1. System and performance characteristics: h_{S0} – static head; h_0 – shutoff head; NOP – normal operating point, AOR – acceptable operating region, BEA – best efficiency area.

A collection of such curves shown in Fig. 3.1.1 by the stroke lines represents the family of the system characteristics for various piping conditions. The system characteristics may change all the time during pumping influenced by a number of variables including variations in fluid viscosity and pumping rate. A designer may have overloaded pump, the piping may corrode, filters and heat exchangers may clog, reservoir levels often alternate, and the pump demand may change.

3.2 Pump properties and performance characteristics

By analogy with piping systems, performance of pumps is primarily given in terms of their flowrate and discharge head.

Every pump has its performance characteristic describing the pump head as a function of the flowrate $h(q)$, while the pump speed, designated as n, is assumed constant:

$$h(q) = h_0 - C_{h1} \cdot q - C_{h2} \cdot q^2,$$ (3.2.1)

where h_0 – pump shutoff head [m],

C_{h1} and C_{h2} – the head friction factors of the pump.

Its graphed representation is called a performance curve or a pump curve.

Pump manufacturers provide the nominal performance characteristics for their pumps as a basis for their exploring. These characteristics are usually given among other passport data in either the polynomial or the graphical form accompanied with a set of characteristic points. They are generated while testing the pump using cold water as liquid. Every passport performance characteristic is fixed for a nominal speed and impeller diameter. This continuously drooping trajectory from the shutoff (no-flow) condition to the maximal flowrate called a nominal operating point (NOP) is shown in Fig. 3.1.1 above the system curves. The pump manufacturer guarantees the nominal flowrate, q_{NOP}, and the corresponding head, h_{NOP}, in NOP. Usually, the NOP is in excess by five to ten percent of the conditions at which the pump will be employed at most of the times or as specified by process demands.

In reality, the pump operates in some accidental pumping working point, [h_N q_N], where the system characteristic intersects the pump performance characteristic. Moreover, pump performance throughout its life often has to take place at some another speed or impeller diameter and service. To this aim, the centrifugal pumping plant usually require a variation of the flowrate or the head and a pump has to adapt to the temporary and permanent changes in process demand. This variation is called as regulation. At regulation, either the system curve or the pump performance curve must be changed to get another working point, [h q], in which the pump flowrate and head generated will differ.

3.3 Affinity laws

To determine approximate performance characteristics at any speed other than the nominal one, *affinity laws* are conventionally used. These laws are based on the Bernoulli's equation, which is, basically, a conservation of energy equation for fluids. The affinity laws are mathematical

expressions that best define changes in the pump flowrate and head when a change is made to pump speed, with all else remaining constant.

The first affinity law determines relationship between the flowrate from the pump and the speed of the pump:

$$\frac{q_i}{q_j} = \frac{n_i}{n_j} \qquad (3.3.1)$$

Here, an index i denotes initial states and index j – new states of the variables.

The second affinity law defines relationship between the head of the pump and the pumping speed:

$$\frac{h_i}{h_j} = \left(\frac{n_i}{n_j}\right)^2 \qquad (3.3.2)$$

Applying the affinity laws to describe the centrifugal pump operation must be done with caution. The general guideline is to use the affinity laws when the system has a friction head dominated upon the static head. In this case, the flowrate varies directly with the speed and the head varies as the square of the speed.

As an example, Fig. 3.3.1 demonstrates a family of pump performance characteristics obtained from the experimental setup. This collection of trajectories for various n is crossed by the system curves represented tiny, thin, average, and thick pipes.
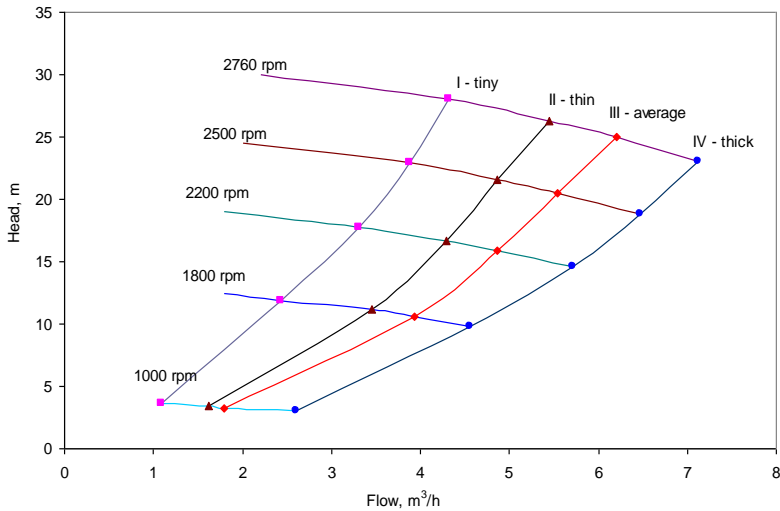
Fig. 3.3.1. Pump performance characteristics at different speed for different pipes.

In addition to the head, energy producing capability of a centrifugal pump is often defined by outlet *pressure*, designated as *p* in this research. In contrast to the head, this property depends on liquid density: it is the mass of liquid processing in the pump by its centrifugal force [8].

By analogy with the head, pressure is split into static pressure and dynamic pressure. The former component is constant whereas the latter one represents a function of the fluid velocity. Total pressure involves both components [9]:

$$p = g\rho\left(h - h_0 - \frac{v^2}{2g}\right), \tag{3.3.3}$$

where ρ – liquid density [kg/m^3],

$\quad\quad g$ – acceleration due to gravity [m/s^2],

$\quad\quad g\rho h$ – pressure at the intake [Pa],

$\quad\quad g\rho h_0$ – pressure at the intake [Pa],

$\quad\quad p_0 = g\rho(h - h_0)$ – static pressure [Pa],

$\quad\quad \rho\frac{v^2}{2}$ – dynamic pressure [Pa],

$\quad\quad v = \frac{q}{A}$ – liquid velocity in a pipeline [m/s],

$\quad\quad A$ – cross-sectional area of the pipe [m^2].

Appropriate system characteristics of pumping system take the form of pressure across the pump as a function of the liquid flowrate [10]:

$$p(q) = p_{S0} + C_p \cdot q^2 \tag{3.3.4}$$

Respectively, pump performance characteristics can be rescaled to pressure:

$$p(q) = p_0 - C_{p1} \cdot q - C_{p2} \cdot q^2 \tag{3.3.5}$$

In this case, the second affinity law describes relationship between outlet pressure and the speed of the pump:

$$\frac{p_i}{p_j} = \left(\frac{n_i}{n_j}\right)^2 \tag{3.3.6}$$

In the pump datasheet, all the pressure data are published, including start-up, shutdown, and upset conditions. As well, the shutoff level restricts maximal pressure a pump will develop under the no-flow condition reflecting a fully blocked outlet [7].

A system power characteristic, $P_s(q)$, demonstrates how system power losses vary with the flowrate:

$$P_s(q) = P_{S0} + C_{PS} \cdot q^3,$$ (3.3.7)

where P_{S0} – system static power [W],

C_{PS} – system friction (dynamic) loss factor [Wm^3/s].

Its graphical representation is called a power loss curve. Unlike the head, the power has a cubical dependence on the flowrate.

The power characteristic of a pump, $P(q)$, and an appropriate power curve describe the pump brake power as a function of the flowrate taking place at a constant pump speed:

$$P_s(q) = P_0 + C_{P1} \cdot q + C_{P2} \cdot q^2,$$ (3.3.8)

where P_0 – pump shutoff power [W],

C_{P1} and C_{P2} – pump loss factor.

The shapes of power curves are dependent on the pump specific speed. Centrifugal pumps of low and medium specific speeds have power curves that rise upward. For higher specific speeds, these curves may be approximately flat and horizontal.

The break powers at different speeds are usually estimated with the help of an appropriate affinity law for power:

$$\frac{P_i}{P_j} = \left(\frac{n_i}{n_j}\right)^3$$ (3.3.9)

This relationship is based on the assumption that system losses remain fixed while transferring from a demanded point on one performance curve to a homologous point on another curve. In real practice, the affinity law for power is not as accurate, especially when the speed change is more than 25 %. If the affinity law for power is used, the computed power requires justification taking into account losses instability. This is the reason why pump manufacturers recommend modifying power equations based on consumer's experience.

3.4 Pump control

3.4.1 Pump regulation by throttling

The most common adjusting device for a constant-speed pump is a control valve in the discharge line, which changes the amount of liquid delivered to the process [11]. The valve takes a pressure drop equal to the difference between pressure supplied by the pump and pressure required by the process. This method is called as regulation by throttling [12]. By throttling, the flow control may be executed.

Because throttling is a mechanical method of the flowrate reduction, various valve angles affect different flowrates and corresponding heads [7]. Throttling changes the system curve by an increase of friction losses. This steepens the system resistance curve with a resultant decrease in flowrate, but the pump performance curve is not altered and the pump continues to operate at full speed.

Thus, this method is recommended mainly when the demanded regulation changes temporary, when the flowrate deviates from the nominal value for short periods of operation [13], mainly on radial pumps that have flatter performance characteristics and better suit for such kind of control. Besides, discharge control valves may be the best choice for lower specific speed pumps (with a rising power curve), on very flat system curves where pumps operate periodically [14].

3.4.2 Pumping speed regulation

In most variable-speed applications, the idea is to use the VSD for slowing the running speed down from the nominal speed. Today, the VSDs are among the front-ranking solutions proposed by Schneider Electric, ABB, Danfoss, and other manufacturers.

Multiple studies have demonstrated the benefits of VSDs in feeding pumps. The method of discharge regulation by varying the pump speed is one of the most economical in view of MEC. With this method, energy to the pump is reduced with the decrease in speed as compared to throttling where full energy is supplied even for a lower operating point. Introducing a VSD to the centrifugal pumping plant allows controlling the pump speed using only electrical energy needed to produce a demanded flowrate. This is similar to applying a new pump with a smaller

impeller [15]. In addition to speed regulation, VSDs improve the controllability of the process and enhance their reliability by minimizing the number of pump switching operations, which improves the pump lifecycle and reduces its maintenance costs [16]. Though the speed control is often more expensive than throttling [13], wear on the pump and valves is less, hence the lifespan of both is generally increased at drooping energy consumption. At this, the pressure level may be reduced, which helps reducing the mechanical stresses generated by throttling devices. Unlike throttling, speed control leaves the piping system characteristic unchanged, while the performance characteristic moves in accordance with the speed change.

3.4.3 Hybrid pump regulation

The hybrid pump and valve combined system topology (Fig. 3.4.1) is offered as an association of two channels – the pump control loop and the valve control loop – fed by a *power management module*. Both the pump VSD and the valve drive get control signals from this power management module, which searches a solution of the consumed power minimisation problem. Individual drive feedbacks are introduced for eliminating offsets caused by the pump speed and valve position instability. An online parameter estimation module is integrated within the proposed framework in order to cope with changing operating conditions.
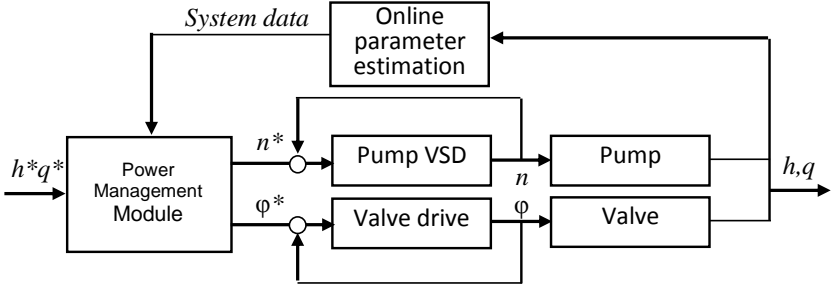
Fig. 3.4.1. Pump regulation with VSD and throttling.

4. SYSTEM LEARNING

This section describes a methodology of receiving metrics from the centrifugal pump system. Received data can be later used in estimation the optimal operation mode for the minimal power consumption and for pump control. Suggested method is not the only possible, but it reduces the amount of work for the engineers who must configure this system. The main reason for using this method is the possibility of its practical application.

This methodology aims to solve the following problems:
1. lack of knowledge about system characteristics, due to the complexity of its measurements;
2. displacement of the optimal operation point of the system consisting of the pump and the drive, from the nominal value of the pump;
3. customer's desire to work outside the nominal areas.

Some of these problems might be solved by using measuring systems of high accuracy. However, these systems are very expensive and they require a lot of maintaining engineer working hours to set up the system. In addition, a full recalculation is required in case of changes in the pipeline system.

4.1 Methodology of system learning

Learning is the first stage of pumping management aiming to receive current information about the system in automatic mode for the future analysis, finding the optimal operation, and pump control. In the case of a centrifugal pumping plant, it is required to measure the flowrate, the head and consumed power in many points, and to compare these points with the drive speed and throttle position.

There are only two possible ways how the user can influence the system operation:
1. to regulate the speed of the pump that allows to move working point in a vertical plane along the system curve (Fig. 4.1.1);
2. to change the throttle position that leads to the change in the system curve whereas the working point will move in a horizontal plane along the performance curve (Fig 4.1.2).

Using these two ways, a learner can estimate all the operating points in the working range. The flowrate, the head (pressure), the motor speed, the valve position, and consumed power have to be measured in every learning point.
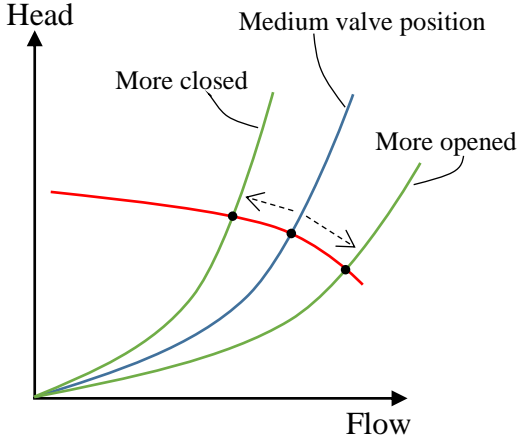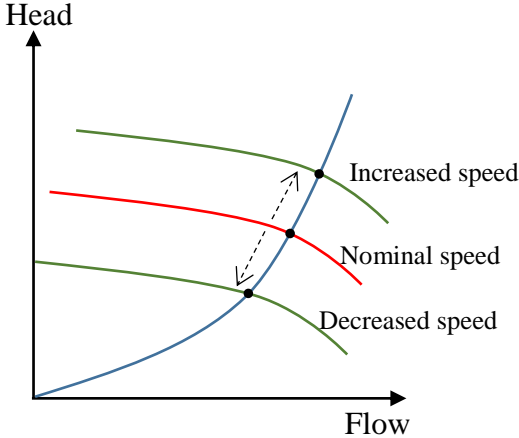
Fig. 4.1.1. Pump control by speed regulation   Fig. 4.1.2. Pump control by throttling

All measurement data are stored in a database for further analysis. The result of the analysis is presented in three tables: the flow tables, the head tables, and the consumed power table at different pump speeds and valve positions. Since the measurements are carried out in semi-automatic mode, it is possible to make measurements with very small steps. This will increase accuracy in finding optimal operating power point.

In case of the absence of the throttling system drive, the only job where an engineer may be involved is to change the throttle angles for entering the angle value to the appropriate table.

One important advantage of this methodology is that it does not require the knowledge of the zero head, which is very problematic for the analytical approach. In addition, it does not require the knowledge of the pump nominal values and many other passport data. Full information comes directly from the real working system. Moreover, this method connects all throttle positions with the system characteristics that cannot be done analytically.

The developed algorithm of learning (Fig. 4.1.3) consists of the following steps:
1. Selecting the speed range at which the pump can still operate. Depending on the manufacture it is ±30-50% of the rated speed; a smaller deviation is allowed at an increased speed.

2. Selecting the permissible measurement speed step. The smaller step will increase the system accuracy, but also will increase the testing time.
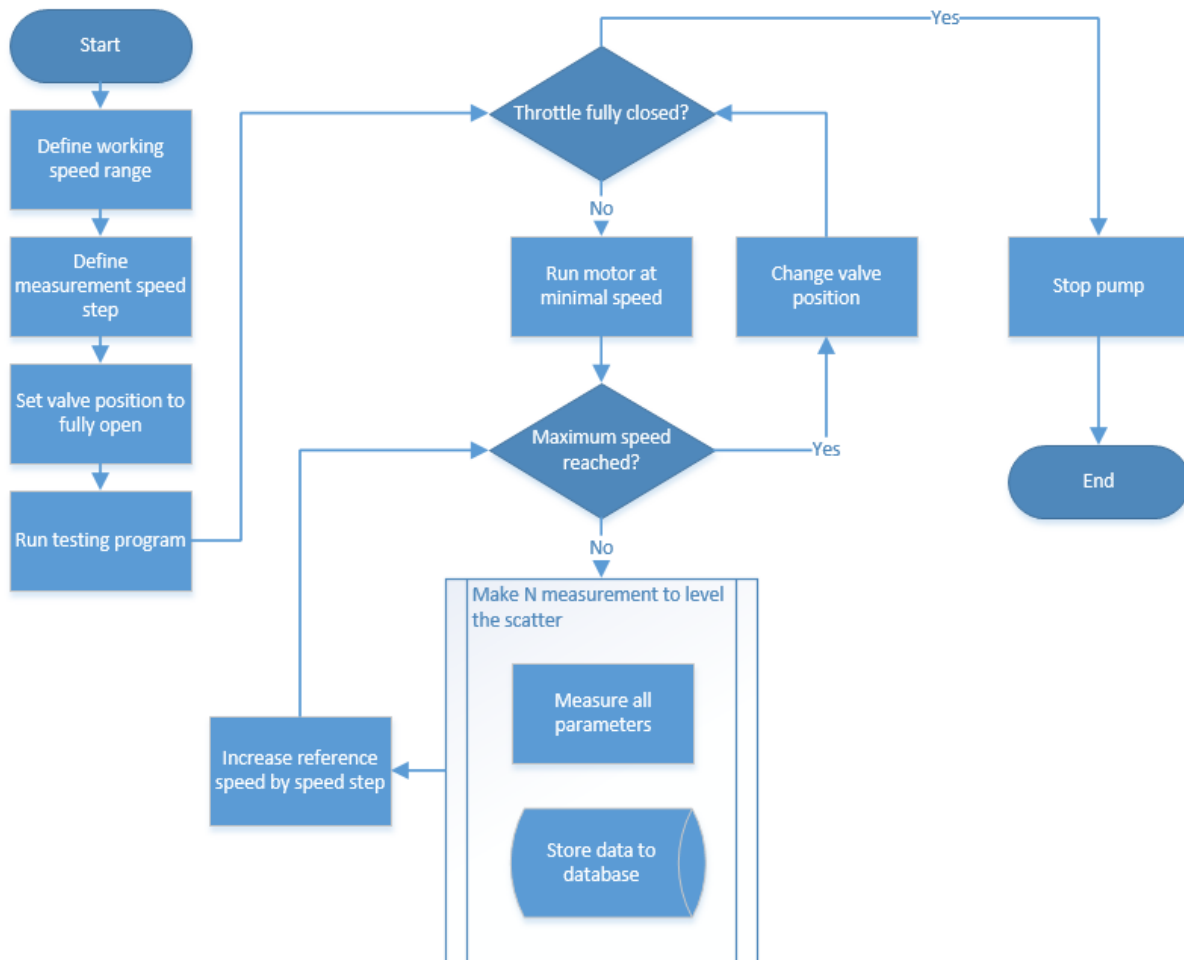
Fig. 4.1.3. A flowchart of the learning program.

3. The throttle position is set to 0 degrees, at which it is considered fully opened.
4. The pump system starts to work and increases the speed from the minimum allowed to the maximum possible value through the measurement steps (Fig. 4.1.4).
5. At each step, it is required to measure the following parameters: consumed power, the head, the flowrate, and pressure. Since the values of these parameters can jump in a certain range, the most rational is to measure all the quantities over time, and to calculate the average value later.
6. When the maximum speed is reached, it is required to set a new throttling angle and to start measurements again. In case when the throttle has its own drive, the system can change the throttling angle itself and enter the new value to the database. Otherwise, the engineer should change the throttle position manually.

7. After completing the full iteration cycle over all the throttle positions (from fully opened to fully closed), the system will get a complete picture of the pump and the pipeline system states.
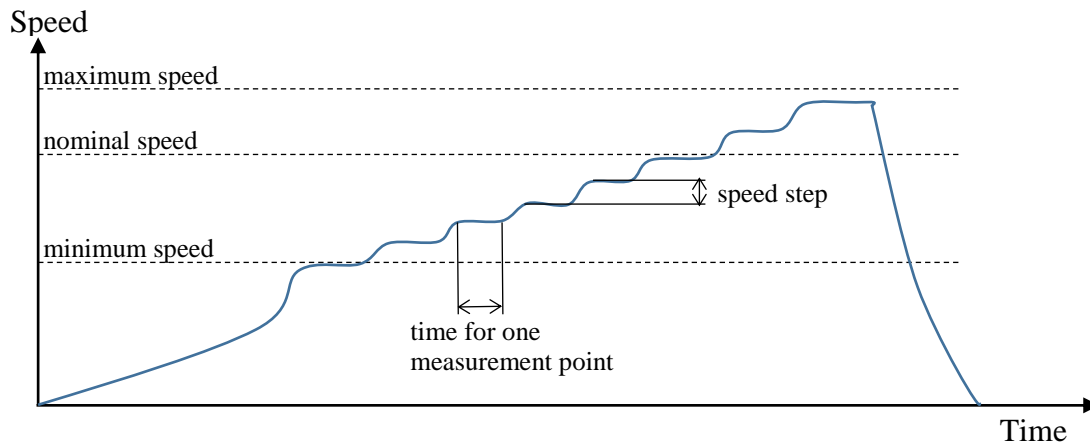
Fig. 4.1.4. Timing diagram of the pump speed during testing for the single throttle position.

With this method, an engineer should also ensure that the motor power does not exceed its maximum allowed level. This problem can occur with a fully opened throttle when the pump is running at the speeds exceeding the nominal values.

4.2 Analytic model

The pump passport characteristics are used for creating the analytic model (Fig. 4.2.1). For the nominal speed 6 points were taken. Those values are presented in Table 4.2.1.

Table 4.2.1. Passport points for the nominal speed.

Q (m³/h)	4.0	5.0	6.0	7.0	8.0	9.0
H (m)	28.3	26.7	25.1	23.8	22.0	21.2
P (kW)	0.80	0.87	0.93	0.99	1.02	1.05

Based on these points, a quadratic function (3.2.1) could be found. To reduce manual computation, the following Excel trendline was used to find resulting pump curve function:

$$H = 47.68 \times Q^{-0.365} \tag{4.2.1}$$

Using affinity laws (3.3.1) and (3.3.2), working points of other performance characteristics may be calculated.
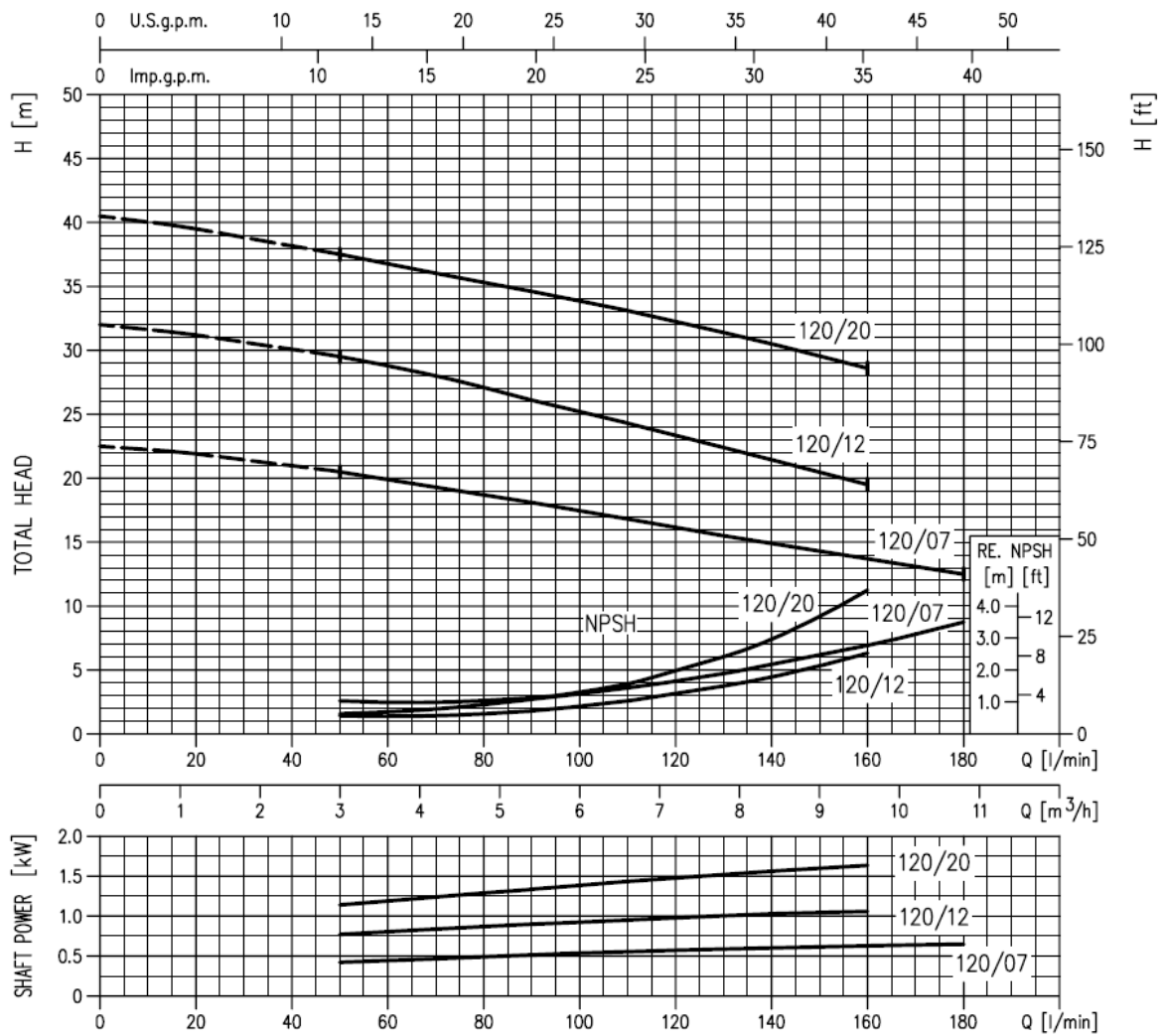
Fig. 4.2.1. Characteristic curves of an Ebara CDX 120/12 series pump provided in the datasheet.

4.3 Implementation of the learning procedure

4.3.1 Experimental setup

An experimental setup (Fig. 4.3.1) designed by ABB and installed in Tallinn University of Technology integrates a set of centrifugal pumps and an embedded pump control software aiming to provide the emulation of the pumping system with its surrounding infrastructure and to enable variation of the physical parameters of the pipeline. The stand contains measuring and control devices and permits real-time process monitoring. Additionally, a PLC and the needed measuring devices were introduced in this research. The software applied involves pump VSD control programs containing the functionalities that are essential and useful for pumping applications for monitoring and adjusting a single pump or a group of pumps. The stand is intended provides a possibility to emulate various situations and phenomena typical for

pumping applications and systems, including challenging situations for identifying the weaknesses of the control methods or malfunctions of the algorithms. [25]

Diagram	Photo
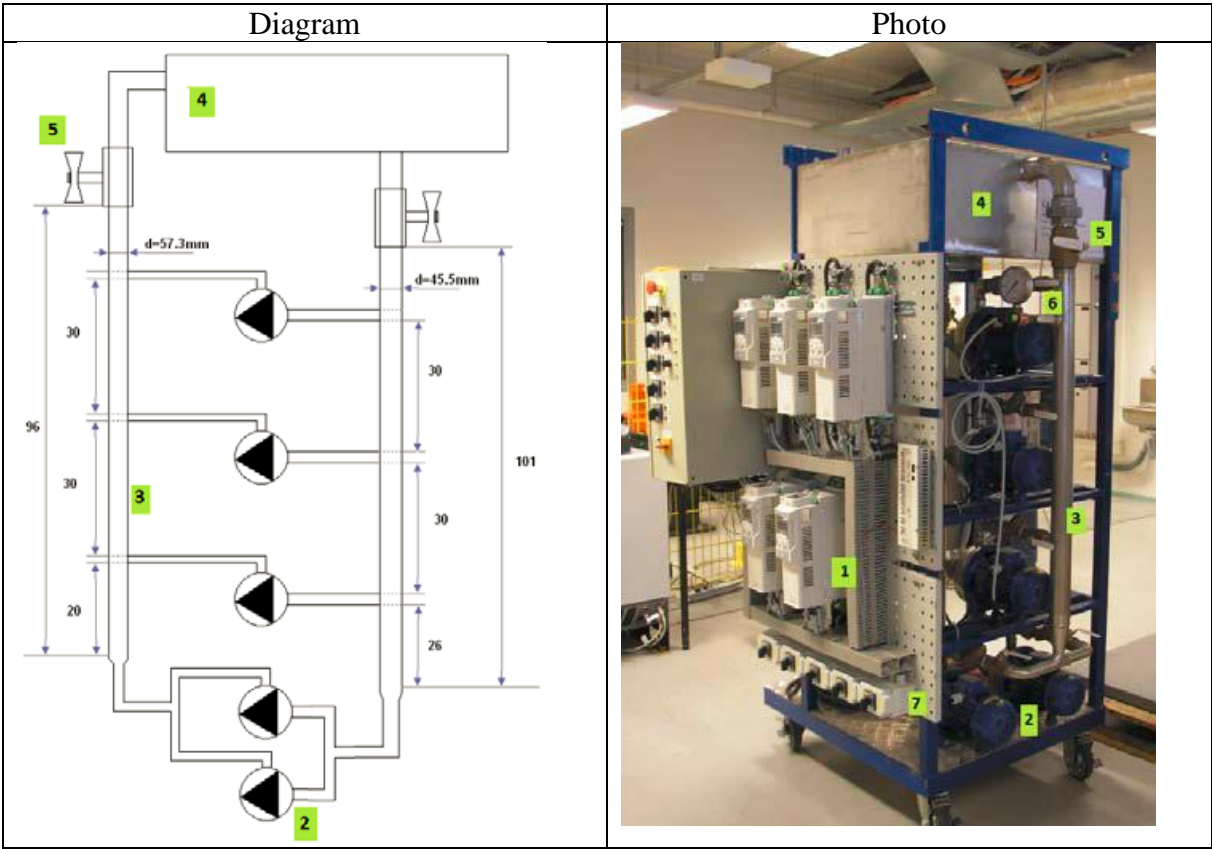
Fig. 4.3.1. Experimental setup: 1 – frequency converter; 2 – centrifugal pump; 3 – pipeline; 4 – water tank; 5 - main throttle; 6 – digital and analogue pressure sensors.

The setup contains five identical centrifugal pumps connected in a parallel network. Each pump is equipped with a separate frequency converter. Specific switching circuitry enables connection of each pump directly to the supply power line or to the corresponding frequency converter. In this way, the pumping systems consisting of variable-speed pumps and non-variable-speed pumps can be emulated. Table 4.3.1 presents nominal data of the pumps and frequency converters. During experimentation, only one pump was used.

Table 4.3.1. Nominal parameters of the pump.

Rated power	1.1	kW
Rated voltage	400	V
Rated current	4.5	A
Rated speed	2760	rpm
Number of poles	2	
Power rating	0.5 ... 2.5	
Protection degree	IP55	

The throttle makes it possible to emulate the variation of demand. Opening the valve emulates a growth of demand and a need in a greater flow from the pumps in order to satisfy it. The stand is implemented as a closed loop system, in which the pipeline starts from a water tank and comes to the same tank installed on the top of the stand. It enables considering the static head during the simulations. Due to the closed-loop architecture, the pressure at the inlet of the pipeline is always constant.

It is equipped with an analogue electronic pressure sensor, though a flowmeter is not installed there. The pressure sensor is connected to the analogue inputs of control boards of all frequency converters. It provides the real-time monitoring of pressure in bars. All the pumps are equipped with ABB ACQ810 frequency converters. Table 4.3.2 contains technical data of the converters.

Table 4.3.2 Nominal parameters of the converter

Rated power	1.1	kW
Rated voltage	400	V
Rated current	3	A
Maximum current	4.4	A

Each frequency converter is equipped with a control board running the modulation process. It can also be used as a powerful process controller. The board is built based on the Texas Instruments 2812 digital signal processor. It includes a circuitry for digital and analogue input/output signals conditioning, RS-232 and RS-485 communication adapters, and flash memory. The converter control board interfaces and connections are shown in Fig. 4.3.2.
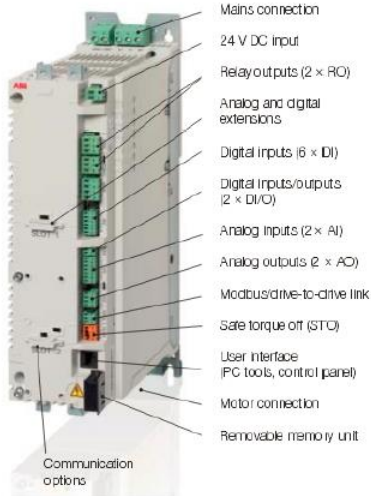
Fig 4.3.2. Interface connection of ACQ810.

The main functions of the control board are as follows to provide the modulation process, to run the drive, to assign the references for the power unit, to adjust pumping, and to set the reference for the speed control functionality.

Generation of the speed reference is implemented based on the readings of the pressure sensor. The most typical speed controller in pumping applications is a PID controller [27]. At that, the inputs of a PID controller are the current values (readings of pressure sensor) and the pressure setpoint, and the output is the speed reference, which is used for speed generation by speed control functionality. The firmware of the converters keeps a wide range of parameters for tuning up the speed controller, the modulation process, the control tools, and process monitoring.

All of these parameters are accessible through the following interfaces:
1. Monitoring and tuning up software "DriveStudio". This software enables real-time monitoring and logging for all the process parameters, speed reference, and modulation. The software is running on the PC and is connected to the frequency converter through the OPC server and RS-232 interface.
2. Various fieldbus protocols that enable acquisition of all the parameters from the frequency converter continuously via a fieldbus master and PLC. The control board of the frequency converter supports embedded Modbus RTU communication functionality. Also, various fieldbus adapters can be mounted onto the control board. ACQ810 supports such fieldbus protocols as Profibus, Device NET, CANopen. In this research, the Modbus\TCP was used to acquire relevant parameters from the converter.

As the drive does not support Modbus\TCP protocol by default, an additional adapter was used the ABB FENA-21 adapter for all Ethernet protocols shown on Fig 4.3.3.

Fig 4.3.3. FENA-21 fieldbus module for Modbus\TCP communication.

Although the drive has a built-in ability to monitor power consumption, an independent source of information about power was introduced. Fluke Power Meter 435 was used as an additional measuring device. Connection of the device is shown on the Fig. 4.3.4.
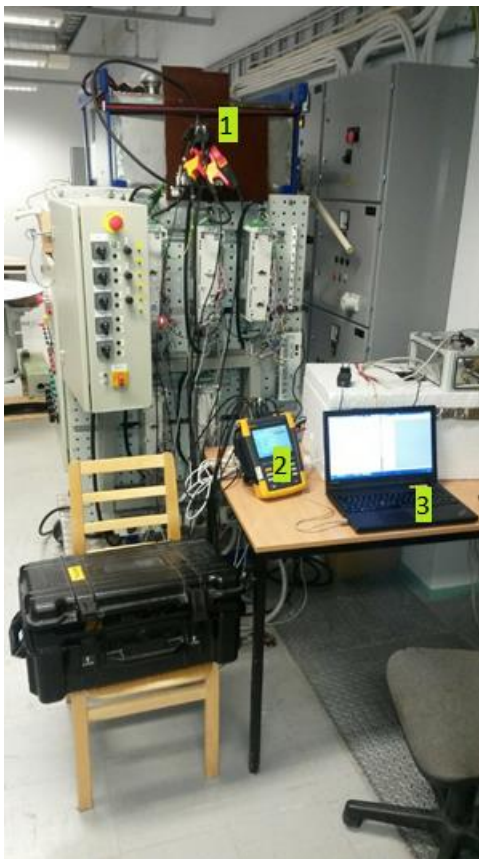
Fig. 4.3.4. Experimental setup with additional power measurement equipment: 1 – power meter delta connected to the input power lines, 2 – Fluke Power Meter 435, 3 – laptop with running learning program.

4.3.2 Learning software

This software provides an opportunity to estimate pump characteristics in the automatic mode. In case of the manual throttle, the learner has to assign the throttle position manually and enter appropriate angle to the database.

The developed learning software is based on following technology stack:

- Python – the main programming language;
- PymodBus – Python module for Modbus\TCP communication;
- SQLite – the database for storing measurements.

Python was chosen as a programming language, because of its wide distribution in scientific community and ease of use. The last point was especially important, since the prototype should be prepared in a shortest possible time and then ported to the CoDeSys program.

4.3.2.1 Drive parameters reading via FENA-21

ACQ810 may read parameters via FENA-21 device and Modbus\TCP protocol. In additional, holding registers acquire actual values of the specified parameters. As an example of the developed software, Listing 4.3.5 demonstrates reading of 32-bit parameters from the drive. As for 16-bit parameters shifting is not required, „reg[0]" always remains empty and „reg[1]" is used only for getting actual values.

Listing 4.3.1. Reading of 32-bit parameters via ModBus.

```
1  def read_parameter_32(register, divider):
2      reg = client.read_holding_registers(register, 2).registers
3      return (( reg[0] << 16 ) + reg[1]) / divider
```

According to the FENA-21 manual, the register address for each drive parameter can be calculated using the following equation:

$$reg_{address} = 20000 + 200 \times P_G + 2 \times P_I - 1, \tag{4.3.1}$$

where $reg_{address}$ – final register address of the parameter,

P_G – parameter group,

P_I – parameter index.

All register values and dividers used during experimentation are shown in Table 4.3.3.

Table 4.3.3. Values for parameter registers.

Name	Parameter	Register	Dimension	Divider
Actual speed	01.01 Motor speed rpm	20201	32-bit	100
Flow	05.05 Flow act	21009	16-bit	100
Flow by head	05.06 Flow by head	21011	16-bit	100
Pressure	02.04 AI1 Scaled	20413	32-bit	1000
Input power	01.22 Power inu out	20243	32-bit	0.001
Motor power	01.23 Motor power	20245	32-bit	0.001

All registers contain values of an integer type. For example, if actual speed is equal to 2100.63 rpm, then the corresponding value in the register is equal to 210063. A divider argument is used in the function to convert a readed value to the desired one. Python does not convert an integer division to the float type by default. For this reason, an additional line is added to the top of the script „from __future__ import division". This line will force Python to convert the result of the integer division to the floating type. In this way, no digits after the comma will be loosed.

4.3.2.2 Database structure

During experimentation all the measurements were stored in the SQLite database for further analysis. The structure of the database can be found in Table 4.3.4.

Table 4.3.4. SQLite database columns structure.

Column name	Type	Description	Example	Unit
Id	INTEGER	Sequence number of measurement.	1	
speed_ref	FLOAT	Reference speed, specified in the program and transferred to the drive via the Modbus\TCP.	2100	rpm
speed_act	FLOAT	Actual speed, readed from the drive at the moment of all other parameters measurement. *Par: 01.01 Motor speed rpm*	2087.95	rpm
Flow	FLOAT	Actual flow as calculated by the drive. *Par: 05.05 Flow act*	2.87	m^3/h
flow_by_head	FLOAT	Flow calculated on the basis of the HQ performance curve. *Par: 05.06 Flow by head*	3.0	m^3/h

Pressure	FLOAT	Pressure value in the output outlet. *Par: 02.04 AI1 Scaled*	1.574	bar
Angle	FLOAT	Throttle valve angle, where with 0 angle throttle is open and with 90 is closed.	80	degree
power_input_drive	FLOAT	System input power, calculated by the drive firmware. *Par: 01.22 Power inu out*	312.1	W
power_motor_drive	FLOAT	Measured motor shaft power, calculated by the drive firmware. *Par: 01.23 Motor power*	273.8	W
power_input_fluke	FLOAT	Measured input power by the Fluke Power Meter.	318.9	W
Timestamp	TIMESTAMP	Time when measurement was done.	2017-03-29 15:46:43	

4.3.2.3 Software initialization

Each start of a program must be followed by special lines. Listing 4.3.2. shows the initialization steps of the program.

Listing 4.3.2. Testing program initialization.

```python
1   from pymodbus.client.sync import ModbusTcpClient as ModbusClient
2   from database import Database
3   from time import sleep
4
5   client = ModbusClient('192.168.0.16')
6   client.connect()
7   template = [
8       ("speed_ref", "FLOAT"),
9       ("speed_act", "FLOAT"),
10      ("flow", "FLOAT"),
11      ("flow_be_head", "FLOAT"),
12      ("pressure", "FLOAT"),
13      ("angle", "FLOAT"),
14      ("power_input_drive", "FLOAT"),
15      ("power_motor_drive", "FLOAT"),
16      ("power_input_fluke", "FLOAT")
17  ]
18
19  db = Database("thesis.sqlite")
20  db.connect("experiment_1", template)
21
22  angle = 0
23  speed_ref_list = range(2100, 3180, 30)
```

Lines 1-3 import all modules that would be used during the program execution.

Lines 5-6 connect the program to the drive by the Modbus\TCP protocol.

In lines 7-1, the database template is defined. The id and timestamp columns are generated automatically at every connection to the database.

In lines 19-20, a database file is created (or is just opened if it already exists) and connected.

In line 22, there is the only one parameter that should be changed manually at each start.

In line 23, an engineer defines, at which speed and how often the measurements would be done. In this example, the measurements are made for each speed from 2100 rpm to 3180 rpm (non-exclusive) with an increasing step equal to 30 rpm.

4.3.2.4 Drive starting and stopping

According to FENA-21 manual, the command to start the drive is 0x47F and the command to stop the drive is 0x47E. All control commands should be sent to the 0 register address. Before sending a start command, it is suggested to send a stop command. Listing 4.3.3 shows two functions to perform this action.

Listing 4.3.3. Drive starting and stopping functions.

```
1  def start_drive():
2      client.write_register(0, 1150)
3      client.write_register(0, 1151)
4
5  def stop_drive():
6      client.write_register(0, 1150)
```

4.3.2.5 Reference speed scaling

A reference speed should be written to the first register address. A reference value of 20000 (4E20h) corresponds to the reference set with the parameter 19.01 Speed scaling. In experimental case, the setting reference value 20000 will be equal to the 4000 rpm reference speed. Listing 4.3.4 shows a function, which converts the desired speed to the correct reference value and sends this command to the drive.

Listing 4.3.4. Reference speed sending to the drive.

```
1  def set_speed_ref(speed_ref):
2      ref_value = int(20000 * speed_ref / 4000)
3      client.write_register(1, ref_value)
```

4.3.2.6 Main cycle

Listing 4.3.5 shows the program main cycle.

Listing 4.3.5. Reading parameters at the different reference speed.

```python
1  start_drive()
2
3  set_speed_ref(2100)
4  sleep(7)
5
6  for speed_ref in speed_ref_list:
7      set_speed_ref(speed_ref)
8      sleep(3)
9
10     for __ in range(50):
11         flow                = read_parameter_16(21009, 100)
12         flow_by_head        = read_parameter_16(21011, 100)
13         pressure            = read_parameter_32(20413, 1000)
14         power_input_drive   = read_parameter_32(20243, 0.001)
15         power_mototor_drive = read_parameter_32(20245, 0.001)
16         speed_act           = read_parameter_32(20201, 100)
17
18         db.commit((speed_ref, speed_act, flow,
19                    flow_by_head, pressure, angle,
20                    power_input_drive, power_motor_drive))
21
22         sleep(0.1)
23
24 stop_drive()
```

Here, the following commands are used:

Lines 1, 24 – drive starting and stopping.

Lines 3, 4 – setting the starting reference speed to 2100 rpm; 7 s delay is added in order the motor could gain the required speed.

Lines 6, 7, 8 – looping over all measured speeds; each speed represents a separate measured point. Measured power from the Fluke Power Meter is added later by parsing its logging file and comparing timestamp with the one in the database.

Lines 10-16 – 50 times reading measurement values; later an average value would be calculated.

Lines 18-20 – measurements inserted to the database.

The total time for estimation of a separate point with 50 probes is 8 second. In experimentation, the measurements were produced for 35 points per each angle, which totally give 287 seconds for teaching the system at one angle. The measurements were made for 8 different angles, what

required slightly less than 40 minutes for defining the full area of pump characteristics. This time might vary depending on the number of required measurement points that, in turn, depend on the required system accuracy.

4.3.2.7 Changes in CoDeSys program

The program has been further converted to the IL code for the AC500 PLC. The following changes were made during porting:

- taking several measurements at one point; PLC did not store the measurements anywhere, but immediately calculated the average value;
- all the measurement points were saved as an array type (not as a table in Python).

4.3.3 Analyzing software

The program described in Listing 4.3.6 is used for reading all the measurements made during the experiment, finding average value for each measurement point, categorizing and dumping the data for subsequent their export to the Excel worksheet.

Listing 4.3.6. Analytic measurements reading program for further study in Excel.

```
1   conn = sqlite3.connect('thesis.sqlite')
2   c = conn.cursor()
3   db_rows = c.execute('SELECT * FROM experiment_1 WHERE angle=?',
4   angle)
5
6   speed_ref_list = range(2100, 3120, 30)
7   speed_values = dict.fromkeys(speed_ref_list)
8   for speed_ref in speed_values:
9       speed_values[speed_ref] = [[], [], [], [], []]
10
11  for _, speed_ref, _, flow, flow_head, pressure, _, _,
12      power_motor_drive, power_input_fluke, _ in db_rows:
13      data = speed_values[speed_ref]
14      data[0].append(power_motor_drive)
15      data[1].append(power_input_fluke)
16      data[2].append(flow)
17      data[3].append(pressure)
18      data[4].append(flow_head)
19
20  print 'Shaft power'
21  for speed_ref, data in sorted(speed_values.iteritems()):
22      print str(sum(data[0]) / len(data[0])).replace('.', ',')
23
24  print 'Power'
25  for speed_ref, data in sorted(speed_values.iteritems()):
26      print str(sum(data[1]) / len(data[1])).replace('.', ',')
27
28  print 'Flow'
```

```
29  for speed_ref, data in sorted(speed_values.iteritems()):
30      print str(sum(data[2]) / len(data[2])).replace('.', ',')
31
32  print 'Pressure'
33  for speed_ref, data in sorted(speed_values.iteritems()):
34      print str(sum(data[3]) / len(data[3])).replace('.', ',')
35
36  print 'Flow by head'
37  for speed_ref, data in sorted(speed_values.iteritems()):
38      print str(sum(data[4]) / len(data[4])).replace('.', ',')
```

In this listing, the following commands are given:

Lines 1-4 – connecting to the database and receiving measurement data.

Lines 6-9 – preparing a structure for storing analyzed data.

Lines 11-18 – categorizing the measurement data by speed.

Lines 20-38 – printing of average value for each speed for one angle as a table column, which can be manually copied to the Excel table.

4.3.4 Experimental results

As a result of the system learning, the following information was obtained:

- a table of consumed power (Table 4.3.5)
- a table of flowrates (Appendix 1)
- a table of pressures (Appendix 2)

As follows from experimentation, once the throttling angle is less than 30 degrees, the data obtained show anomalies. One of the probable reasons is poor sensor location: when the throttle was fully opened, the pressure in the pipe was not pumped properly. As a result, the pressure sensor showed data close to zero, and, since many other data are based on the pressure sensor measurements, they are proved insufficient as well. Another probable reason relates to a cavitation phenomenon. The only data that can be trusted for given angles are the amount of consumed power, because their measurement was done independently of the main experiment. However, it was decided to exclude these data from the future work. Thus, we only have measurements for 5 different valve positions.

A system and pump curves for nominal values are displayed on the Fig 4.3.5. Equation 3.3.3 was used to convert measured pressure to the head level. It is clearly seen how pressure sensors stopped working at small angles.
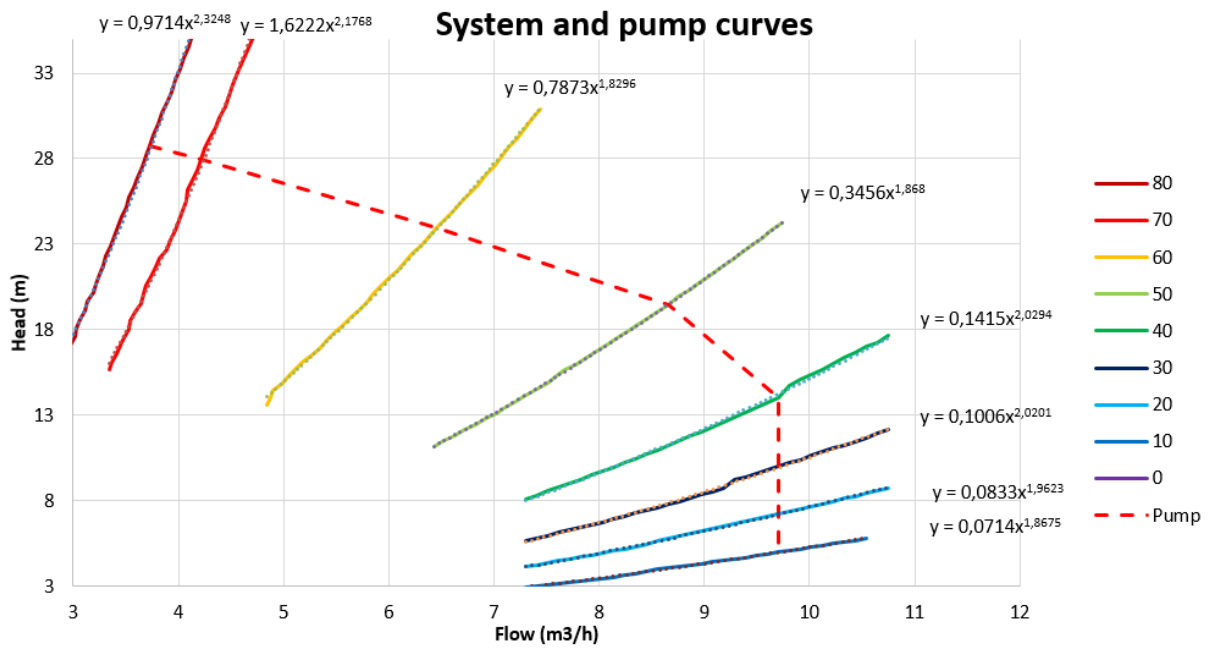
Fig 4.3.5. Estimated system and pump curves at different throttling angles for nominal speed.

Table 4.3.5. System input power at different speed and throttle angles

Speed (rpm)	Angle (degrees)							
	80	70	60	50	40	30	20	10
2100	318,9	341,1	418,3	462,7	499,4	521,9	532,5	540,5
2130	331,6	354,5	435,6	481,4	519,6	542,5	554,3	562,8
2160	344,4	368,6	453,3	500,3	540,6	565,0	577,1	585,1
2190	358,0	383,0	471,2	520,0	562,3	587,1	600,2	608,1
2220	371,6	398,0	489,0	540,3	583,5	610,7	623,6	632,7
2250	386,1	412,8	508,2	561,2	606,6	634,3	647,6	657,5
2280	400,2	428,6	527,4	582,4	629,6	657,7	672,6	683,4
2310	414,5	444,4	546,8	604,3	653,6	683,1	698,5	709,3
2340	429,3	460,4	567,3	626,4	678,5	709,1	724,6	736,6
2370	444,9	476,9	588,0	649,9	703,1	734,7	751,6	763,6
2400	460,7	494,2	609,1	673,2	728,5	761,8	778,7	794,3
2430	476,9	511,6	631,0	697,7	755,9	788,3	808,3	826,9
2460	493,5	529,4	652,7	722,5	782,0	818,3	841,3	856,4
2490	509,7	547,6	675,7	748,0	809,6	847,1	870,8	884,5
2520	527,1	566,3	699,0	773,7	838,4	876,2	903,3	918,3
2550	544,1	584,8	722,6	800,4	867,2	907,1	934,8	950,0
2580	562,2	604,3	747,2	827,3	896,5	937,8	967,4	979,4
2610	580,7	624,2	771,7	854,9	926,3	969,4	1000,5	1016,1
2640	599,0	644,7	797,2	883,2	957,3	1003,0	1034,3	1047,6
2670	618,0	665,0	822,8	912,4	989,7	1043,0	1066,9	1084,5
2700	637,8	686,3	849,4	941,9	1022,9	1077,8	1101,9	1118,8
2730	657,3	708,0	876,0	971,8	1054,9	1112,9	1137,9	1157,0
2760	677,5	729,8	903,9	1002,9	1088,2	1147,8	1171,9	1193,5
2790	698,7	752,4	932,3	1034,1	1122,9	1183,8	1212,3	1229,6
2820	719,2	775,2	961,0	1066,7	1165,5	1221,7	1252,3	1271,4
2850	740,6	798,9	990,0	1100,3	1202,7	1260,8	1288,3	1307,0
2880	762,6	822,6	1020,4	1133,5	1239,9	1298,9	1329,0	1353,4
2910	784,6	846,3	1050,4	1166,9	1276,9	1337,2	1371,9	1395,3
2940	807,2	871,3	1081,7	1202,4	1315,0	1378,7	1410,6	1434,1
2970	830,2	897,1	1113,4	1237,6	1354,6	1422,3	1452,1	1479,0
3000	853,7	922,9	1146,1	1274,0	1393,9	1464,8	1495,9	1523,6
3030	877,9	948,5	1179,0	1311,7	1434,9	1506,3	1543,6	1568,9
3060	902,1	974,9	1212,5	1349,6	1477,2	1550,9	1587,8	1615,1
3090	927,8	1002,3	1247,1	1388,1	1521,1	1596,0	1638,3	1665,5
3120	953,0	1030,1	1282,6	1427,5	1565,0	1643,9	1684,9	
3150	978,7	1058,3	1318,3	1468,8	1610,7			
3180	1005,1	1086,8	1354,8					

4.4 Comparison of the experimental and analytical models

To be confident that the measured values are correct, all the data were validated by the affinity laws. The results can be seen in Tables 4.4.1, 4.4.2 and 4.4.3.

Table 4.4.1. Affinity law for the power

$\left(\dfrac{n_{max}}{n_{min}}\right)^3$	$\dfrac{P_{max}}{P_{min80}}$	$\dfrac{P_{max}}{P_{min70}}$	$\dfrac{P_{max}}{P_{min60}}$	$\dfrac{P_{max}}{P_{min50}}$	$\dfrac{P_{max}}{P_{min40}}$	$\dfrac{P_{max}}{P_{min30}}$	$\dfrac{P_{max}}{P_{min20}}$	$\dfrac{P_{max}}{P_{min10}}$
2.915	2.677	2.706	2.740	2.753	2.791	2.807	2.809	2.819

Table 4.4.2. Affinity law for the flow

$\dfrac{n_{max}}{n_{min}}$	$\dfrac{Q_{max}}{Q_{min80}}$	$\dfrac{Q_{max}}{Q_{min70}}$	$\dfrac{Q_{max}}{Q_{min60}}$	$\dfrac{Q_{max}}{Q_{min50}}$	$\dfrac{Q_{max}}{Q_{min40}}$	$\dfrac{Q_{max}}{Q_{min30}}$	$\dfrac{Q_{max}}{Q_{min20}}$	$\dfrac{Q_{max}}{Q_{min10}}$
1.429	1.381	1.352	1.445	1.453	1.429	1.429	1.429	1.429

Table 4.4.3. Affinity law for the head

$\left(\dfrac{n_{max}}{n_{min}}\right)^2$	$\dfrac{H_{max}}{H_{min80}}$	$\dfrac{H_{max}}{H_{min70}}$	$\dfrac{H_{max}}{H_{min60}}$	$\dfrac{H_{max}}{H_{min50}}$	$\dfrac{H_{max}}{H_{min40}}$	$\dfrac{H_{max}}{H_{min30}}$	$\dfrac{H_{max}}{H_{min20}}$	$\dfrac{H_{max}}{H_{min10}}$
2.041	2.057	2.069	2.028	2.004	2.054	2.024	1.985	1.905

It can be concluded from the tables that the obtained data are reliable and can be used for future optimization and control procedures.

To further compare the experimental and analytical models a plot with both pump curves shown in Fig 4.4.1 was introduced. As can be seen from the graph, the measured data almost completely coincide with the passport data in the range where the pressure sensor worked properly. However, with the opened valve, the sensor did not show correct results, which led to an increase in the error in this region. In addition, there is increased gap as soon as the pump speed exceeded the nominal.

To calculate the deviation value the following formula was used:

$$error = 1 - \frac{H_{nom}}{H_{meas}}, \tag{4.4.1}$$

where $error$ – deviation of the measured value from the nominal value,

H_{nom} – nominal head received from the motor passport for selected flow,

H_{meas} – measured head.

The resulting deviations were entered to Table 4.4.4 and displayed graphically in Fig 4.4.2.
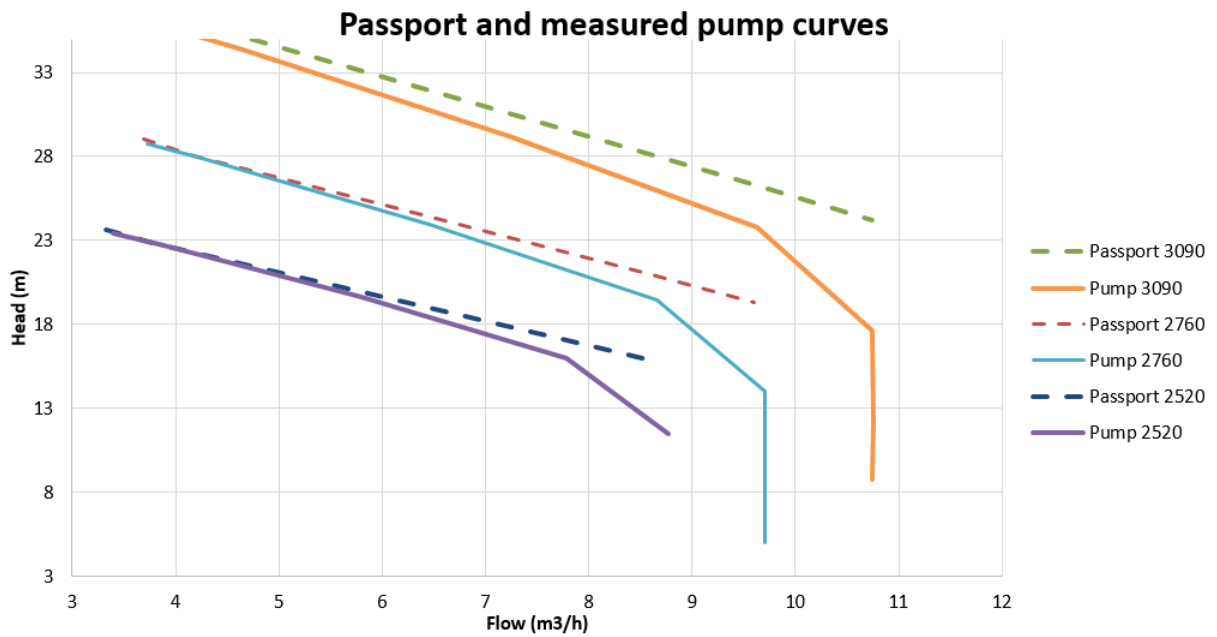
Figure 4.4.1. Estimated centrifugal pump performance curves comparing with the curves obtained from the pump passport for different speed.

Table 4.4.4. Deviation of the estimated flow-head characteristic from the passport characteristic.

Q	3,689	4,185	6,384	8,564	9,600	9,598	9,600	9,598
H_{nom}	29	28	24,5	21	19,3	19,3	19,3	19,3
error	0,007938	0,001476	0,023331	0,072008	0,274273	0,481909	0,626216	0,741426
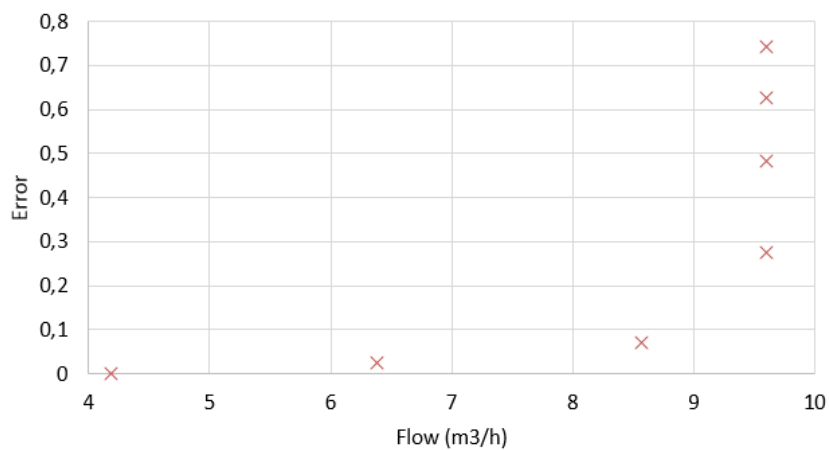
Fig 4.4.2. Deviation of the measured head from the nominal value at different flows.

5. TABULAR METHOD OF A SEARCH OF POINTS WITH MINIMAL POWER CONSUMPTION

5.1 Methodology of tabular method

The developed tabular method is based on the lookup tables that represents data sets with all possible operating states of the centrifugal pumping plant. Creation of this tables was described in Chapter 4 as a result of pump system learning. Once learning was completed, three tables appeared in the system memory: the consumed power table, the flowrate table, and the pressure table (could be converted to head). All lookup tables have a dependence on the position of the throttle and on the speed of the centrifugal pumping plant. The system can store several similar lookup tables created at different system characteristics both in the program memory, and on the hard drive or external drive in the form of files that may be read at request. Since that lookup tables exist, the next management step is to find the optimal operation point where consumed power will be minimal.

First, the engineer has to assign an area in which the pump is able to perform properly without cavitation. This area is usually restricted by the minimum and maximum possible flowrate and pressure (or head). It is also possible to set the desired parameters, and assign additionally permissible parameter deviations.

Once the working area is specified, a developed algorithm (Fig. 5.1.1) starts the search of the optimal operation point. First, all the accessible points are sorted into an array in such a way that their order on the system-pump graph goes from left to right, from bottom to top. If consumed power appears to be equal in some points, this ranged set will allow automatic choosing the point with greater hydraulic power. Initial parameters are then initialized and the program starts iterating over the values in the lookup tables. If the speed and flow in an ith point meets the permissible speed (n^*) and flowrate (q^*) constraints and its consumed power is less than the value of a temporary variable, this point will be selected as the optimal operation point. In turn, if the points appear with equal or very close consumed power values (regarding the permissible power gap), the point will be choosen where the hydraulic power has the highest value.

As soon as the last row in the lookup table is scanned, the temporary variable finally keeps optimal operation point. After that, the reverse operation is performed for the chosen point – the search for the pump speed and the throttle angle where this point was obtained.
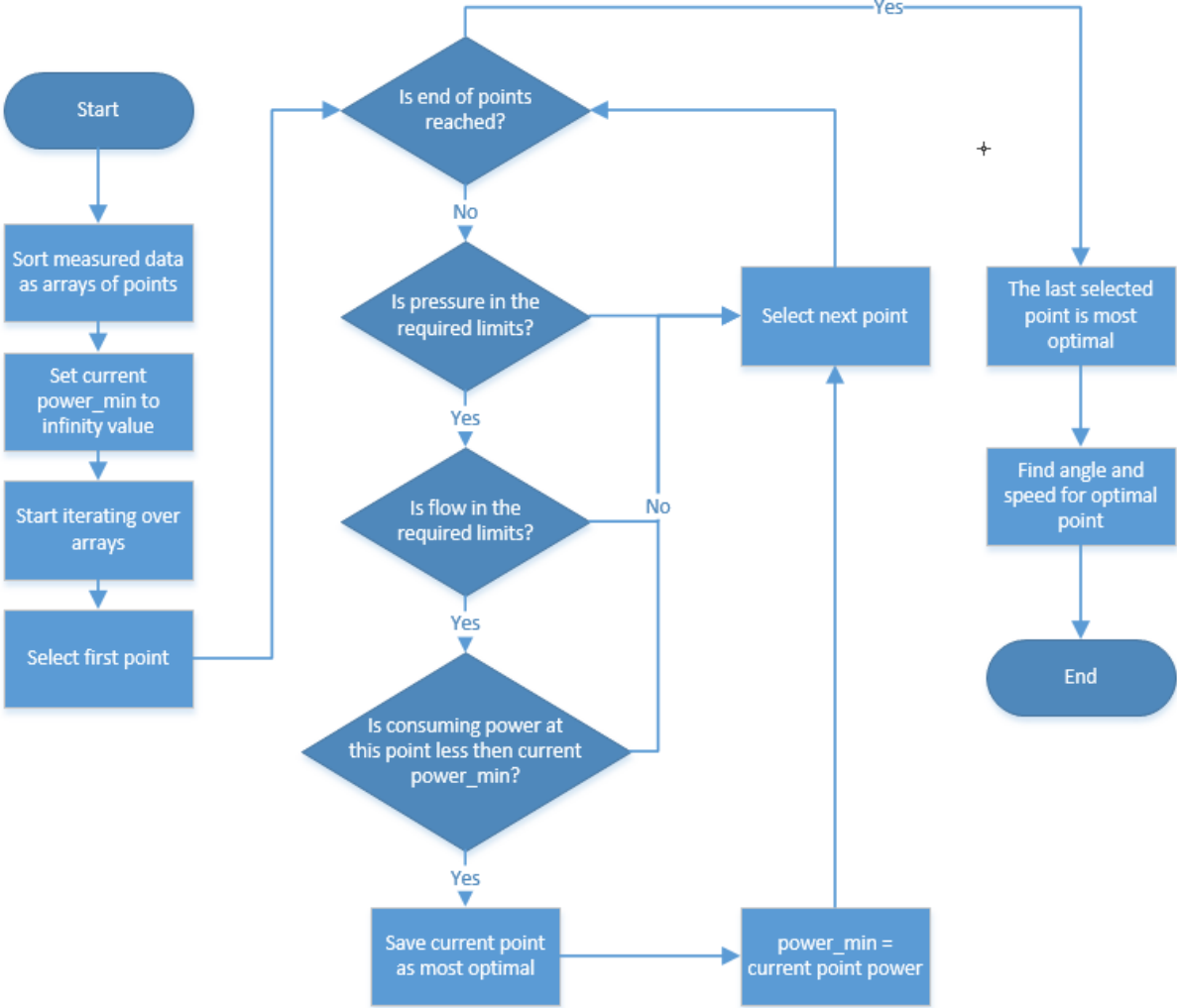
Fig. 5.1.1. Flowchart of the tabular method of an optimal operation point search.

The developed tabular method has the following advantages:
- it is based on the real estimated data;
- it is simple;
- in case of condition change, the lookup tables may be rebuild and the system will continue its performance;
- though the method is used for the consumed power minimization, it, however, can also be applied for other optimizations, such as minimal energy consumption, highest efficiency search, highest hydraulic power search, etc.

However, the following limitations exist:

- only discrete points can be selected;
- to get accurate results, it is necessary to learn the system using a very small measured step, which in turn leads to learning time increase;
- accuracy of this method depends on accuracy of measurements and on the number of measurements.

5.2 Implementation of the tabular method

Listing 5.2.1 demonstrates a fragment of the developed algorithm implementation program.

Listing 5.2.1. A function for getting an optimal point by the tabular method.

```
1   def get_optimal_speed_and_angle(p_min, p_max, q_min, q_max,
2                                    speed_list, speed_list_size,
3                                    angle_list, angle_list_size,
4                                    power_list,
5                                    preassure_list,
6                                    flow_list):
7
8       power_min = 999999
9       power_min_index = 0
10      opt_speed = 0
11      opt_angle = 0
12
13      for i in range(speed_list_size * angle_list_size):
14          if (preassure_list[i] >= p_min and
15              preassure_list[i] <= p_max and
16              flow_list[i] >= q_min and
17              flow_list[i] <= q_max):
18
19              if power_list[i] <= power_min:
20                  power_min = power_list[i]
21                  power_min_index = i
22
23      for i in range(speed_list_size):
24          for j in range(angle_list_size):
25              if (i * angle_list_size + j) == power_min_index:
26                  opt_speed = speed_list[i]
27                  opt_angle = angle_list[j]
28
29      return (opt_speed, opt_angle)
```

The following commands comprise the program:

Lines 8-11 – parameters initialization.

Lines 13-21 – lookup table iteration for finding i, with smallest consuming power.

Lines 23-27 – reverse operation aimed to find a throttle angle and pump speed for the operation point found.

Line 29 – returning the optimal values of the pump speed and the throttle angle.

5.3 A search of the optimal point in experimental setup

To test the method, several regions were selected. The result of the method for this regions are shown in Table 5.3.1. Throttle angle (φ^*) and pump speed (n^*), as output, marked by grey background.

Table 5.3.1. The result of tabular method for different regions.

N	p_{min}	p_{max}	q_{min}	q_{max}	φ^*	n^*
1	2.5	3.0	3.0	5.0	80	2520
2	1.0	2.5	2.0	6.0	20	2100
3	1.6	2.4	5.0	8.0	60	2340
4	2.0	2.4	5.0	8.0	50	2550
5	2.0	2.6	5.0	8.0	60	2610
6	2.0	3.0	3.0	7.0	80	2370

The problem encountered during algorithm testing was the insufficiently small measurement step taken for the angles. If the range has a too narrow limits for the flow, it was easy to get into the zone where measurements were absent, either where points for only one angle were measured. The result is issued as a discrete value of angle and speed.

6. TABULAR-ANALYTICAL METHOD OF SEARCHING FOR OPTIMAL POINT WITH MINIMAL POWER CONSUMPTION

6.1 Methodology of the tabular-analytical method

The advantage of tabular method lies in its experimental base. Measured data from the real system are used in the search for optimal operation point procedure. At the same time, there is no need for any additional computations based on theoretical knowledge or assumptions. However, the drawback of the method is its discreteness – it is possible to work only in those points where the system measurements were made. For high system accuracy, it required to make a huge number of measurements in the learning stage which become too long and not always possible. The method efficiency dramatically drops if very narrow ranges are specified. A situation aggravates when experimental points in the specified area are absent or when their number is too small for selection.

Learning may be replaced with calculation based on the analytical model proceeded from the passport data using the pump and pipeline characteristics in the form of equations and the laws of affinity. This approach might allow to find the flowrate and the head or pressure at any point as well as to find the pump speed in this point. Unfortunately, analytical method looses its accuracy upon the pump and pipeline parameter variations.

The proposed below tabular-analytical method combines both approaches. Primary based on the tabular method, which allows mapping the system state through experimental learning, it includes an analytical part, allowing finding intermediate values between the points estimated by learning.

In this research, two tabular-analytical methods were developed based on linear interpolation:
- a method for the corner points search, which allows finding an optimal pump operation when the measured points in a given head-flow range are absent;
- a method for the points search within a given head-flow range taking into account the measurements at the nearby points.

6.2 Bilinear interpolation

Linear interpolation is the way to calculate the intermediate value of a function from two already known values. Bilinear interpolation is an extension of linear interpolation for the grid.
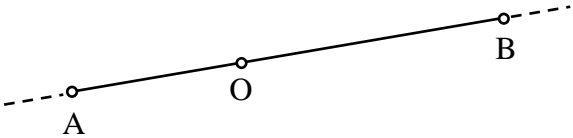
Fig. 6.2.1. Finding of O point from known A and B points.

Let us assume that the values and coordinates at some points A and B are known (Fig. 6.2.1). In this case it is possible to find a value at any point O on a given line using the following equation:

$$\frac{O-A}{B-A} = \frac{AO}{AB},$$
(6.2.1)

where   O – searched value at point O,
        A – known value at point A,
        B – known value at point B,
        AO – a length of the line between A and O points,
        AB – a length of the line between A and B points.

In case of the coordinate grid, this equation is transformed as follows:

$$O = (B-A) \times \sqrt{\frac{(O_x-A_x)^2+(O_y-A_y)^2}{(A_x-B_x)^2+(A_y-B_y)^2}} + A,$$
(6.2.2)

Any item can be used as a value for points: a flowrate, a head, pressure, a pump speed, a throttle angle, consumed power, efficiency, hydraulic power, etc.

In the case of bilinear interpolation, power is searched in the auxiliary points P and E (Fig. 6.2.2). It is possible to draw a straight line through those points, so that O would belong to this line. To simplify calculation, the auxiliary line is chosen perpendicular to the flowrate axis.
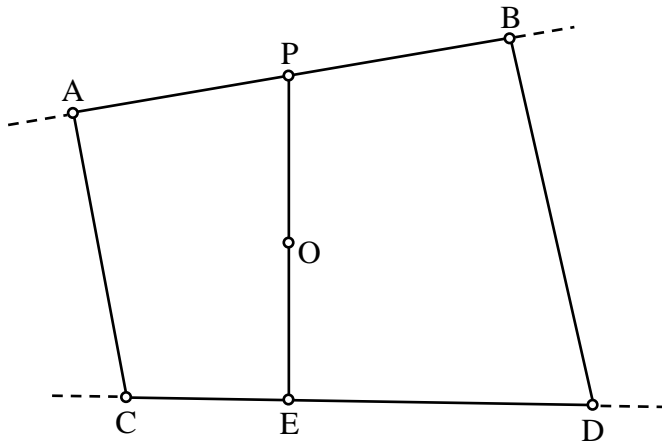
Fig 6.2.2. Finding the value at point O with bilinear interpolation from four points.

To estimate power at point O, the following steps have to be performed:

1. Finding the Y coordinate of the auxiliary points.
2. Finding power at the auxiliary points using linear interpolation.
3. Finding power at the desired point using linear interpolation with auxiliary points.

6.3 Tabular-analytical method for corner points

Using bilinear interpolation, power at any corner point is accessible as well as the throttle angle and the pumping speed. Although these values appear as a result of theoretical calculations, they are all based on experimental data.

The method for corner points works properly if there are no points inside the given range or only one point exists. In this case, it is assumed that the optimal working point will be in one of the four corner points (or one of the five points if there is one inside). This approach is based on the assumption of the linear change in the values between adjacent points.
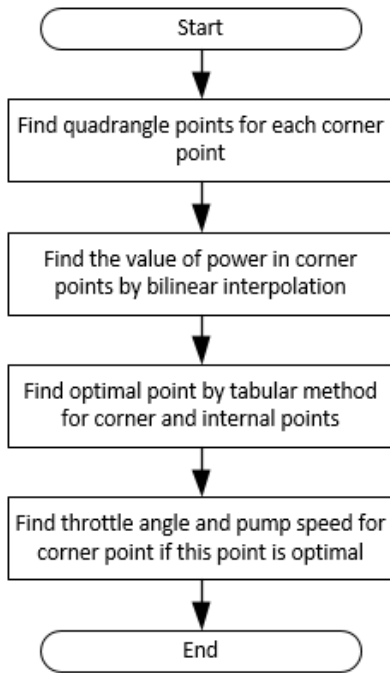
Fig. 6.3.1. Flowchart of finding an optimal point using corner points.

In order to estimate power or any other required quantity (throttle angle, pump speed, etc.) at the corner points, first it is required to find four points for each rectangle vertex, so that the formed quadrangle would include the desired point (Fig. 6.3.1). A quadrangle was chosen as a basis for interpolation in this method, because of ease of finding its points (Fig. 6.3.2).
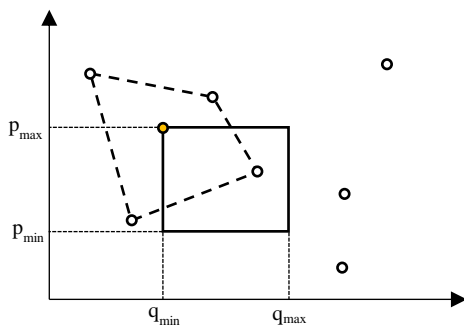
Fig. 6.3.2. Selecting of four measured points to find a corner value.

Once power is found in all corner points, it becomes possible to use a tabular method for them (including one internal point, if available). When the optimal point will be found, it is possible to find the value of the throttle angle and the pump speed similar with the bilinear interpolation.

6.4 Program implementation of the tabular-analytical method for corner points

Using (6.2.2), Listing 6.4.1 was developed. This function takes *x* and *y* coordinates of the desired point where it is required to find necessary values, and takes array of points those values are already known.

Listing 6.4.1. Function for the bilinear interpolation.

```python
 1  def bilinear_interpolation(x, y, points):
 2      (A_x, A_y, A), (B_x, B_y, B), (C_x, C_y, C), (D_x, D_y, D) =
 3  points
 4
 5      P_x = x
 6      P_y = ((x - A_x) * (B_y - A_y)/(B_x - A_x)) + A_y
 7
 8      E_x = x
 9      E_y = ((x - C_x) * (D_y - C_y)/(D_x - C_x)) + C_y
10
11      AP = math.sqrt(math.pow(P_x - A_x, 2) + math.pow(P_y - A_y, 2))
12      AB = math.sqrt(math.pow(B_x - A_x, 2) + math.pow(B_y - A_y, 2))
13
14      CE = math.sqrt(math.pow(E_x - C_x, 2) + math.pow(E_y - C_y, 2))
15      CD = math.sqrt(math.pow(D_x - C_x, 2) + math.pow(D_y - C_y, 2))
16
17      P = (B - A) * (AP / AB) + A
18      E = (D - C) * (CE / CD) + C
19
20      return ((P - E) * (y - E_y)/(P_y - E_y)) + E
```

This function includes the following commands:

Lines 2-3 – points disclosure resulting in coordinates for A, B, C and D, and their values.

Lines 5-9 – finding the coordinates of the auxiliary points.

Lines 11-15 – finding the length of segments for linear interpolation of auxiliary points.

Lines 17-18 – finding the value at the auxiliary points.

Line 20 – returning the result of linear interpolation for the desired point.

Following this function, the tabular method can be applied for found points to find an optimal working point.

6.5 A search of an optimal point in experimental setup using the tabular-analytical method for corner points

To test a method, the same regions were selected as for the tabular method. In this case, operation points may be find for those experiments were not made. The results of the algorithm implementation are shown in Table 6.5.1. Graphical representation of the selected regions is shown on Fig. 6.5.1 taking into account only corner points.

Table 6.5.1. Calculated throttle angle and pump speed for different operation regions.

	Tabular-analytical method for corner points						Tabular method	
N	p_{min}	p_{max}	q_{min}	q_{max}	φ^*	n^*	φ	n
1	2.5	3.0	3.0	5.0	73.0	2436	80	2520
2	1.0	2.5	2.0	6.0	13.2	1624	20	2100
3	1.6	2.4	5.0	8.0	69.5	2316	60	2340
4	2.0	2.4	5.0	8.0	50.2	2450	50	2550
5	2.0	2.6	5.0	8.0	64.3	2560	60	2610
6	2.0	3.0	3.0	7.0	73.0	2436	80	2370

Here, the darkest color corresponds to a lower power consumption, whilst the white one is the largest power consumption. The blue dot displays the operation point of the centrifugal pump, which was selected by the algorithm. It is seen that in all cases the point is located in one of the corners, although in some cases it would be possible to pick any other point in a certain range.

Therefore, the tabular-analytical method for corner points is suitable for successful selection the throttle angle and the operation speed of the pump for each of the operation regions.
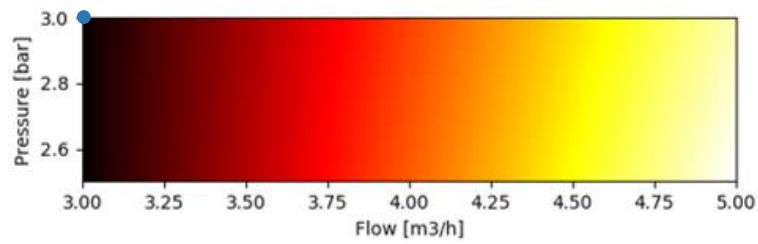
$\varphi^* = 73.0\ °$
$n^* = 2436$ rpm
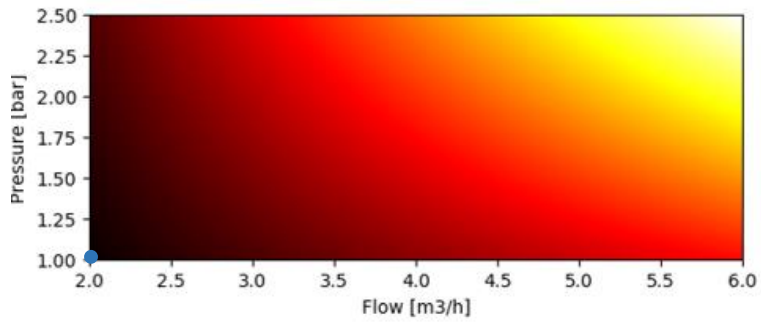
$\varphi^* = 13.2\ °$
$n^* = 1624$ rpm
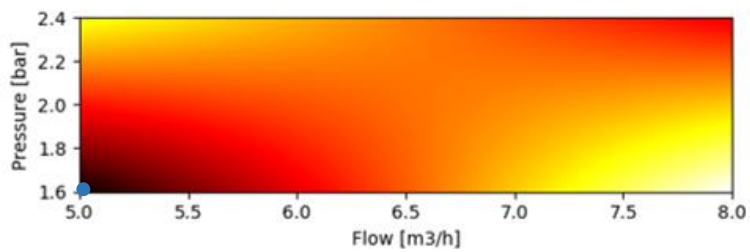
$\varphi^* = 69.5\ °$
$n^* = 2316$ rpm
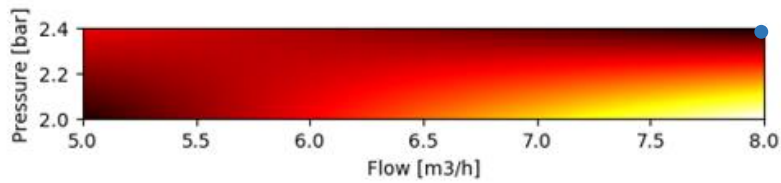
$\varphi^* = 50.2\ °$
$n^* = 2450$ rpm
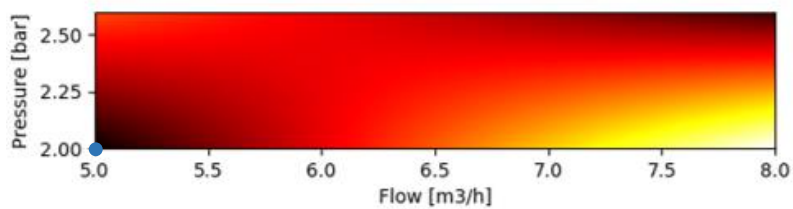
$\varphi^* = 64.3\ °$
$n^* = 2560$ rpm
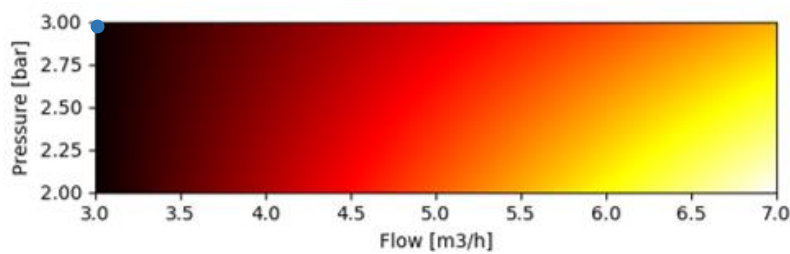
$\varphi^* = 73.0\ °$
$n^* = 2436$ rpm

Fig. 6.5.1. Visualization of the optimal operation point selection based on corner points.

51

6.6 Tabular-analytical method for all points

In a tabular method, it is possible to find the optimal working point only for those positions where the measurements were made ignoring the fact that any possible optimal point may lie somewhere between them.

In the tabular-analytical method for corner points, all interior points are ignored assuming that the optimal point is in one of its corners. A particularity of this method is its discreteness: the choice of a working point is produced only among the corner points without taking into account internal points. However, the obtained plots might be strongly changed if additional points appear within the range.

The tabular-analytical method for all points appeared as a development of the previous method. At this approach, all the previous disadvantages are removed and it is possible to find the values at all points within a specified limit, taking into account all the measured points. For the corner points, interpolation occurred for the chosen quadratic. To make it possible taking into account all points, it is necessary to use interpolation for triangles, since they can cover the entire desired plane regardless of the number of points on it.
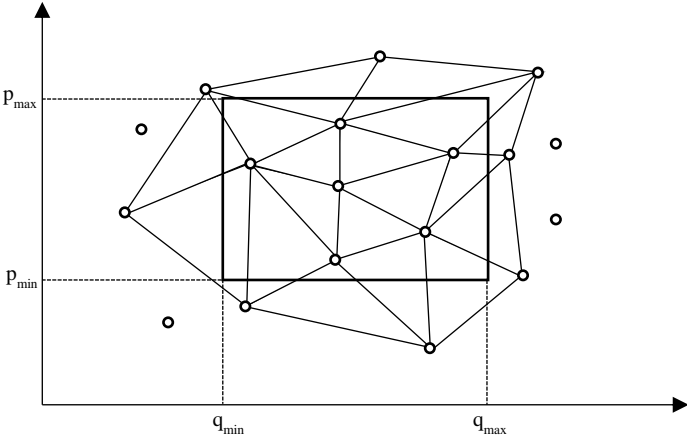
Fig 6.6.1. Triangulation of plane with the limitation rectangle.

Fig. 6.6.1 shows the triangulation of points for a given range. Triangulation should be carried out until the entire rectangle of limits is covered. Later it will be possible to calculate the required value at any point inside the triangle.

It is also necessary to know the value at the auxiliary point (but only for one point in this case) to calculate the value inside the triangle. A desired point will belong to the line drawn from one vertex of the triangle to the opposite side (Fig. 6.6.2). The position of the auxiliary point P is found in an intersection of two line function f_{AO} and f_{BC}. Then a value can be found by linear interpolation.
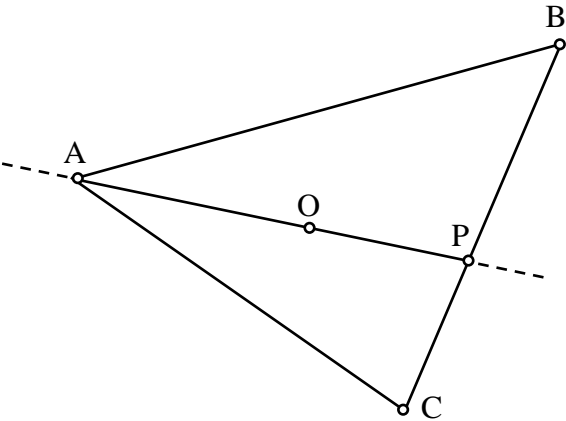
Fig. 6.6.2. Points position in case of bilinear interpolation for triangles.

When the value at the auxiliary point is received, it is possible to find a value at any point on the given line, including the desired point, using (6.2.2). In this case, only one auxiliary point will be used whereas the others are obtained experimentally.

With this approach, it is possible to calculate the value at any point on the pump-system characteristics graph. Taking into account all measured points assuming linear variation of values between these points. Although this relation usually has non-linear nature, an error of this assumption is expected to be less than an error of the measurement instruments.

To search for the optimal point, all points within the specified limit are studied. In this case, not only the measured points are selected, but all the points at the regular intervals.

```
                    ┌───────────────┐
                    │     Start     │
                    └───────────────┘
                            │
              ┌─────────────────────────────┐
              │  Make plane triangulation    │
              │  and write all triangles to  │
              │  array.                      │
              └─────────────────────────────┘
                            │
            ╱─────────────────────────────╱
           ╱  qmin, qmax, pmin, pmax,    ╱
          ╱   p=pmin, q=qmin           ╱
         ╱─────────────────────────────╱
```

Start

Make plane triangulation and write all triangles to array.

q_{min}, q_{max}, p_{min}, p_{max}, $p = p_{min}$, $q = q_{min}$

Find triangle for p and q

Interpolate P_m at (p,q) point and save value to new array

$q = q + \Delta q$

$q > q_{max}$

No

Yes

$p = p + \Delta p$
$q = q_{min}$

$p > p_{max}$

Yes

Find optimal point in new array with tabular method

Interpolate throttle angle and pump speed for the optimal point

End

Fig. 6.6.3. Algorithm of finding an optimal point using a tabular-analytical method by analyzing all points in the specified range.

An advantage of the method is the possibility of finding an optimal point among many points in the specified range. In addition, there is no longer need to make a detailed learning. It is possible to run learning stage with a higher step still maintaining sufficient flexibility of the system. Comparing to the purely analytical method, this is based on an experimental basis, which improves its performance in practical work. As well, it provides a possibility to find the operating modes of the pump among any number of points without complex calculations and accurate measuring devices.

However, the disadvantage of this method is a larger number of calculations, which can slow down the system in cases when it is required to find the optimal point too often.

6.7 Program implementation of the tabular-analytical method for all points

The first stage of the program is the division of the plane into triangles. The code of the functions that allows achieving these results is shown on Listing 6.7.1.

Listing 6.7.1. Triangulation of the plane limited by a rectangle.

```
1   def add_to_triangle(point, triangle, triangles):
2       triangles.remove(triangle)
3       triangles.append((point, triangle[0], triangle[1]))
4       triangles.append((point, triangle[1], triangle[2]))
5       triangles.append((point, triangle[2], triangle[0]))
6
7   def delaunay_triangulation(limits, points):
8       p1, p2, p3, p4 = limits
9       triangles = [(p1, p3, p4), (p1, p2, p4)]
10
11      for point in points:
12          for triangle in triangles:
13              if is_triangle_inside(point[0], point[1], triangle):
14                  add_to_triangle(point, triangle, triangles)
15                  break
16
17      return triangles
```

The code includes the following commands:
Lines 1-5 – a function for adding three triangles instead of one.

Lines 8-9 – limits disclosure and initial triangle making.

Lines 11-15 – adding of every point to the triangulation; for each point there is a triangle in which it is located divided into three smaller ones.

Line 17 – returning of an array of triangles for this plane.

The next stage is the iteration of the points within the limits. For each point, it is required to find a triangle, which will cover this point. Listing 6.3.1.2 shows a function used to check if point is located in the triangle.

Listing 6.7.2. Function to check if the desired point is located in the triangle.

```
1   def is_triangle_inside(x, y, triangle):
2       (a_x, a_y, __), (b_x, b_y, __), (c_x, c_y, __) = triangle
3
4       alpha = (((b_y - c_y)*(x - c_x) + (c_x - b_x)*(y - c_y)) /
5               ((b_y - c_y)*(a_x - c_x) + (c_x - b_x)*(a_y - c_y)))
6
7       beta = (((c_y - a_y)*(x - c_x) + (a_x - c_x)*(y - c_y)) /
```

```
8                  ((b_y - c_y)*(a_x - c_x) + (c_x - b_x)*(a_y - c_y)))
9
10      gamma = 1.0 - alpha - beta
11
12      if alpha > 0 and beta > 0 and gamma > 0:
13          return 1
14      elif alpha == 0 or beta == 0 or gamma == 0:
15          return 2
16      else:
17          return 0
```

The function includes the following commands:

Line 2 – points disclosure to get coordinates of the points at the vertex of the triangle.

Lines 4-10 – finding the coefficients of vector multiplication.

Lines 12-17 – returning of the verification result:

> 1 – point is inside the triangle;
>
> 2 – point is on the edge of the triangle;
>
> 0 – point is outside the triangle.

At the last stage, it is necessary to find the power value at the desired point. For this reason, a bilinear interpolation for triangle is used. Listing 6.7.3 shows implementation of the interpolation function.

Listing 6.7.3. A function of bilinear interpolation for triangle form.

```
1   def bilinear_interpolation_triangle(x, y, points):
2       (a_x, a_y, a), (b_x, b_y, b), (c_x, c_y, c) = points
3
4       E_y = ((x*a_y - y*a_x)*(b_x - c_x) - (x - a_x)*(b_x*c_y -
5   b_y*c_x)) / ((x - a_x)*(b_y - c_y) - (y - a_y)*(b_x - c_x))
6       E_x = ((x*a_y - y*a_x)*(b_y - c_y) - (y - a_y)*(b_x*c_y -
7   b_y*c_x)) / ((x - a_x)*(b_y - c_y) - (y - a_y)*(b_x - c_x))
8
9       BE = math.sqrt(math.pow(E_x - b_x, 2) + math.pow(E_y - b_y, 2))
10      BC = math.sqrt(math.pow(c_x - b_x, 2) + math.pow(c_y - b_y, 2))
11
12      E = (BE/BC) * (c - b) + b
13
14      AO = math.sqrt(math.pow(x - a_x, 2) + math.pow(y - a_y, 2))
15      AE = math.sqrt(math.pow(E_x - a_x, 2) + math.pow(E_y - a_y, 2))
16
17      return (AO/AE) * (E - a) + a
```

The function includes the following commands:

Line 2 – points disclosure resulting in coordinates for points A, B and C and their values.

Lines 4-7 –finding the coordinates of the auxiliary E point.

Lines 9,10,14,15 – finding the length of segments for linear interpolation.

Line 12 – finding the value at the auxiliary point.

Line 17 – returning the value at the desired point.

As soon as an array of new points is received, a tabular method can be applied to find the optimal working point.

6.8 A search of an optimal point in experimental setup using the tabular-analytical method for all points

For testing reason, the same regions were chosen as for other methods. The results of the method for finding the optimal operation point taking into account all points is shown in Table 6.8.1 and in Fig. 6.8.1.

Table 6.8.1. Calculated throttle angle and pump speed for different operation regions

Tabular-analytical method for all points							Method for corner points		Tabular method	
N	p_{min}	p_{max}	q_{min}	q_{max}	φ^*	n^*	φ	n	φ	n
1	2.5	3.0	3.0	5.0	69.3	2247	73.0	2436	80	2520
2	1.0	2.5	2.0	6.0	13.4	1918	13.2	1624	20	2100
3	1.6	2.4	5.0	8.0	68.9	2386	69.5	2316	60	2340
4	2.0	2.4	5.0	8.0	64.4	2610	50.2	2450	50	2550
5	2.0	2.6	5.0	8.0	64.4	2624	64.3	2560	60	2610
6	2.0	3.0	3.0	7.0	63.8	1936	73.0	2436	80	2370

It is clear from the obtained data that the optimal operation point has moved to the center of the region. The reason was a higher samples of points and taking into account the error of power measurements. As a result, the program choses a point with a higher hydraulic power still having the lowest power consumption category.
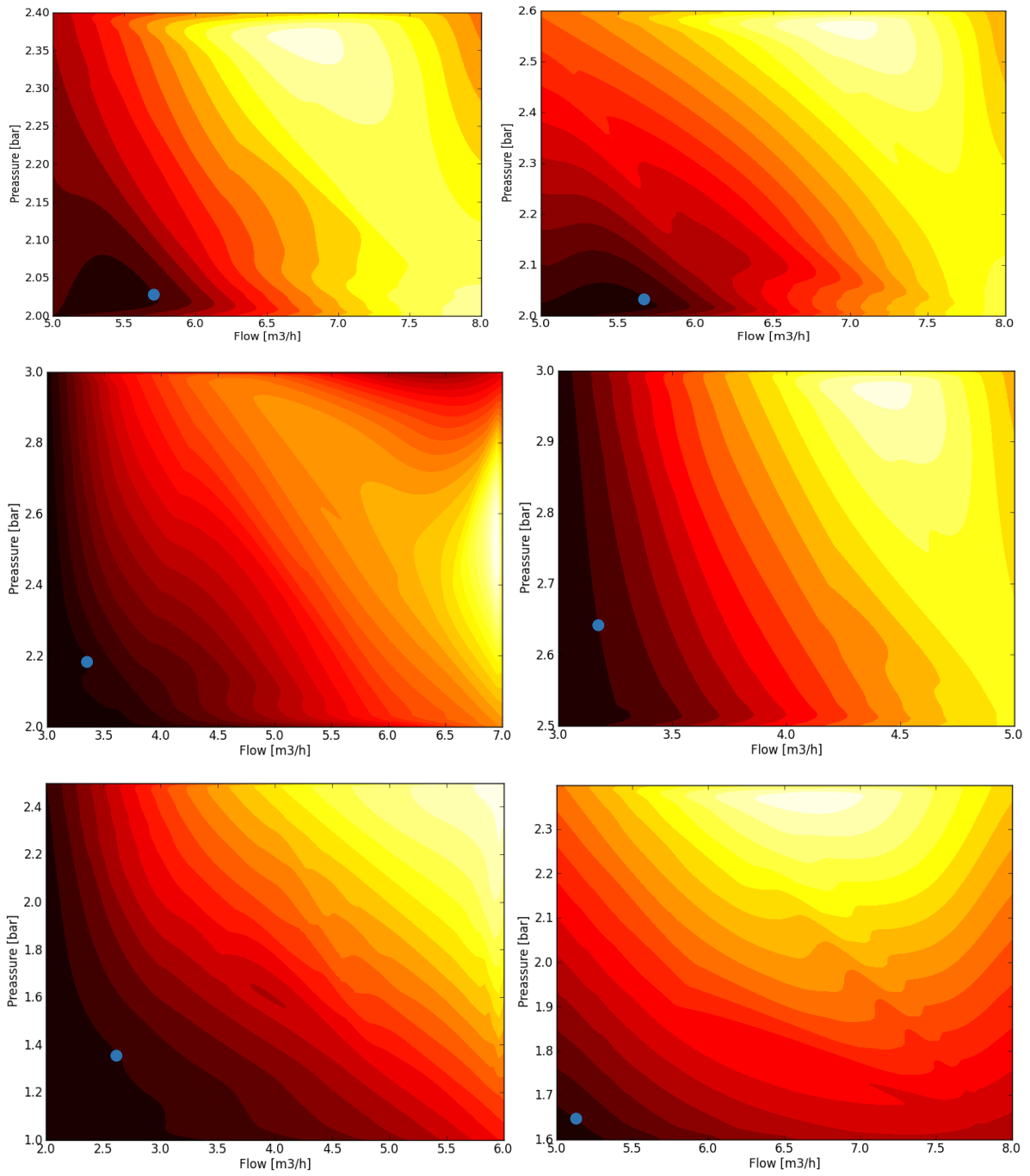
Fig. 6.8.1. Visualization of the optimal operation point selection for all points.

7. CONCLUSIONS

In this study, the author succeeded in presenting the methodology for power management of the centrifugal pump.

A methodology and an application for the automatic learning of the centrifugal pump model was developed. As a result of the learning process, the lookup tables were created that contain various data (pressure, flow, and consumed power presented in this thesis) tied to the controlled system parameters – throttle angle and pump speed. The data in the lookup tables were used to find the optimal operation point of the centrifugal pump where the minimum power is consumed from the supply grid.

A family of algorithms was developed to find the optimal operation point of pumping using the data collected with the help of learning. All algorithms are presented in the form of the Python programs that can easily be converted to any programming language. The algorithms developed by the author seek an optimal point where the minimal power is consumed. However, it is possible to apply these algorithms to other parameters, such as the highest efficiency of the system, highest hydraulic power, minimal energy consumed, etc.

The new power management methodology represents an instrument for carrying out both pressure and flowrate adjustments independently or simultaneously using mutual throttling and speed control. In contrast to the traditional pumping at which either the demanded flowrate or demanded pressure is fixed, the developed hybrid system opens the possibility for optimal energy management within a permitted pressure-flow area, including the modes when both the demanded flow and pressure are assigned together.

All the developed algorithms were tested on a real experimental setup, and experimental data are presented in this thesis.

The results of this research have a high practical value. The methodology described in the thesis was developed primarily for the purpose of its further implementation as a module for pumping applications. From the theoretical point of view, this research may be considered as a study of the possibility and feasibility of centrifugal pumps to operate both inside and outside the nominal areas.

For a further practical implementation, it is necessary to rewrite the programs presented in the thesis for the appropriate pump. If ACQ810 drive is used, then the entire program can be written as a separate application on top of a main program and installed in the drive desired by the user. The advantage of this approach is that only relatively inexpensive pressure sensors are needed for normal operation. The flowrate and the head can be calculated analytically by the system itself. If the program should work outside the drive, it is possible to implement this solution for the PLC. In this case, some additional steps for calculation or measuring the flow in the pipes should be taken.

Although the thesis includes the ready-to-used completed programs, there exist many opportunities to enhance the developed approach. For example, a specified setup may be prepared to improve the learning methodology by covering the working area with measured points more extensively. As well, it makes sense to improve the triangulation algorithm, since the used one has enough low quality of partitioning.

In the author's opinion, all targets and tasks that were set for the thesis research were fully complied, and the results are ready for implementation by the end users.

BIBLIOGRAPHY

1. Key World Energy Statistics, OECD/IEA, 2016, 80 p.

2. I. Annus, D. Uibo and T. Koppel, "Pumps energy consumption based on new EU Legislation," Procedia Engineering, Elsevier, vol. 89, 2014, pp. 517 – 524.

3. Pump Applications for the TWT Deposit Control System. Available at: https://www.triangularwave.com/PumpProtectionFactSheet.htm (18.04.2017)

4. Tracking Industrial Energy Efficiency and CO2 Emissions, OECD/IEA, 2007, 324 p.

5. D. E. Agthe, R. B. Billings and N. Buras (Eds.), Managing Urban Water Supply, Springer Science & Business Media, 2013, 277 p.

6. H. M. Badr and W. H. Ahmed, Pumping Machinery Theory and Practice, John Wiley & Sons, 2015, 388 p.

7. K. Fernandes, B. Pyzdrowski, D. W. Schiller and M. B. Smith, Understand the basics of centrifugal pump operation, CEP magazine, May 2002, pp. 52 – 56.

8. J. R. Pottebaum, Optimal characteristics of a variable-frequency centrifugal pump motor drive, IEEE Transactions on Industry Applications, IA-20 (1), Jan./Feb. 1984, pp. 23 – 31.

9. Grundfos Industry Pump Handbook, 160 p.

10. H. A. Wiegand and L. B. Eddy, Characteristics of centrifugal pumps and compressors which affect the motor driver under transient conditions, Transactions of the American Institute of Electrical Engineers, Part II: Applications and Industry, 79 (3), Jul. 1960, pp. 150 – 156.

11. M. Al-Khalifah and G. K. McMillan, Control valve versus variable speed drive for flow control, ISA InTech Magazine, Jul./Aug. 2013, pp. 1 – 11.

12. S. Shiels, When trimming a centrifugal pump impeller can save energy and increase flow rate, World Pumps, Nov. 1999, Elsevier, pp. 37 – 40.

13. Centrifugal Pump Handbook, Sulzer Pumps, Elsevier, 2010, 283 p.

14. A. R. Budris, Selecting the Best/Most Efficient Centrifugal Pump Control, Water World, Comcast, 7 p.

15. H. Vasquez, J. Parker and T. Haskew, Control of a 6/4 switched reluctance motor in a variable speed pumping application, Mechatronics, 15, Elsevier, 2005, pp. 1061 – 1071.

16. O. Alarfaj and K. Bhattacharya, Power consumption modeling of water pumping system for optimal energy management, IEEE, 2016, pp. 1 – 5.

17. Ilja Bakman, High-Efficiency Predictive Control of Centrifugal Multi-Pump Station with Variable Speed Drives, TUT Press, 2016.

18. ABB ACQ810 Firmware Manual: ABB Oy.

19. Gevorkov, L., Vodovozov, V. and Lehtla, T. (2015). PLC-based flow rate control system for centrifugal pumps.− 2015 56th International Scientific Conference on Power and Electrical Engineering of Riga Technical University (RTUCON): Latvia, Riga: 239-243.

APPENDIX

The value of the flow (m³/h) at each measurement points found experimentally

Speed (rpm)	Angle (degrees)							
	80	70	60	50	40	30	20	10
2100	2,909	3,338	4,841	6,430	7,303	7,304	7,303	7,302
2130	2,941	3,371	4,873	6,522	7,408	7,409	7,409	7,408
2160	2,974	3,417	4,901	6,624	7,514	7,513	7,513	7,517
2190	3,022	3,449	4,987	6,722	7,617	7,618	7,618	7,616
2220	3,033	3,482	5,049	6,825	7,721	7,721	7,722	7,722
2250	3,068	3,524	5,115	6,919	7,826	7,827	7,825	7,826
2280	3,117	3,545	5,178	7,023	7,929	7,930	7,932	7,933
2310	3,141	3,587	5,270	7,107	8,035	8,033	8,035	8,034
2340	3,194	3,645	5,349	7,208	8,139	8,139	8,138	8,139
2370	3,211	3,664	5,411	7,296	8,243	8,244	8,243	8,243
2400	3,247	3,687	5,478	7,406	8,348	8,348	8,348	8,346
2430	3,285	3,738	5,563	7,505	8,452	8,453	8,451	8,452
2460	3,313	3,780	5,633	7,585	8,557	8,556	8,555	8,555
2490	3,351	3,819	5,719	7,671	8,660	8,662	8,662	8,660
2520	3,393	3,888	5,798	7,779	8,765	8,767	8,765	8,765
2550	3,429	3,924	5,852	7,880	8,869	8,869	8,868	8,870
2580	3,463	3,975	5,919	7,975	8,974	8,975	8,975	8,974
2610	3,501	4,000	6,007	8,067	9,076	9,077	9,077	9,078
2640	3,535	4,036	6,083	8,172	9,184	9,183	9,182	9,182
2670	3,573	4,073	6,158	8,267	9,288	9,286	9,286	9,287
2700	3,614	4,091	6,228	8,367	9,393	9,390	9,392	9,389
2730	3,652	4,134	6,315	8,467	9,495	9,494	9,497	9,496
2760	3,689	4,185	6,384	8,564	9,600	9,598	9,600	9,598
2790	3,722	4,210	6,457	8,659	9,705	9,703	9,704	9,705
2820	3,767	4,248	6,538	8,750	9,806	9,808	9,809	9,809
2850	3,812	4,295	6,617	8,857	9,912	9,912	9,912	9,914
2880	3,847	4,350	6,691	8,950	10,017	10,018	10,017	10,017
2910	3,893	4,391	6,769	9,053	10,122	10,121	10,121	10,121
2940	3,940	4,448	6,854	9,143	10,224	10,224	10,228	10,223
2970	3,975	4,483	6,915	9,247	10,330	10,331	10,332	10,330
3000	4,016	4,514	6,996	9,344	10,434	10,435	10,435	10,434
3030	4,054	4,560	7,071	9,441	10,542	10,539	10,541	10,538
3060	4,101	4,605	7,143	9,538	10,643	10,644	10,643	10,643
3090	4,134	4,654	7,225	9,633	10,749	10,749	10,748	10,747
3120	4,174	4,703	7,286	9,741	10,852	10,851	10,852	
3150	4,229	4,756	7,361	9,836	10,954			
3180	4,261	4,801	7,442					

The value of the pressure (bar) at each measurement points found experimentally

Speed (rpm)	Angle (degrees)							
	80	70	60	50	40	30	20	10
2100	1,5798	1,5264	1,3149	1,0656	0,7541	0,5148	0,3656	0,2486
2130	1,6248	1,5719	1,3597	1,0964	0,7741	0,5273	0,3733	0,2537
2160	1,6718	1,6172	1,4012	1,1260	0,7955	0,5406	0,3840	0,2593
2190	1,7201	1,6645	1,4412	1,1564	0,8162	0,5564	0,3945	0,2650
2220	1,7691	1,7119	1,4801	1,1870	0,8367	0,5691	0,4046	0,2709
2250	1,8189	1,7592	1,5214	1,2174	0,8600	0,5833	0,4135	0,2783
2280	1,8679	1,8069	1,5614	1,2488	0,8815	0,5995	0,4230	0,2842
2310	1,9197	1,8570	1,5999	1,2820	0,9043	0,6131	0,4342	0,2896
2340	1,9698	1,9065	1,6412	1,3145	0,9274	0,6314	0,4452	0,2960
2370	2,0218	1,9580	1,6840	1,3486	0,9504	0,6446	0,4552	0,3035
2400	2,0735	2,0093	1,7246	1,3804	0,9724	0,6600	0,4659	0,3150
2430	2,1272	2,0604	1,7680	1,4150	0,9961	0,6755	0,4770	0,3269
2460	2,1813	2,1137	1,8100	1,4509	1,0197	0,6881	0,5008	0,3340
2490	2,2353	2,1645	1,8532	1,4884	1,0453	0,7064	0,5135	0,3391
2520	2,2893	2,2156	1,8982	1,5209	1,0693	0,7229	0,5255	0,3478
2550	2,3452	2,2689	1,9437	1,5560	1,0939	0,7384	0,5369	0,3552
2580	2,4012	2,3232	1,9882	1,5926	1,1178	0,7578	0,5509	0,3617
2610	2,4581	2,3806	2,0315	1,6279	1,1421	0,7694	0,5602	0,3702
2640	2,5147	2,4382	2,0778	1,6642	1,1689	0,7904	0,5761	0,3767
2670	2,5734	2,4941	2,1247	1,7012	1,1950	0,8373	0,5870	0,3851
2700	2,6307	2,5533	2,1715	1,7394	1,2223	0,8540	0,5966	0,3906
2730	2,6912	2,6108	2,2187	1,7768	1,2472	0,8739	0,6111	0,4004
2760	2,7504	2,6687	2,2664	1,8155	1,2751	0,8908	0,6212	0,4075
2790	2,8116	2,7291	2,3152	1,8539	1,3013	0,9082	0,6350	0,4168
2820	2,8715	2,7893	2,3630	1,8949	1,3739	0,9280	0,6486	0,4228
2850	2,9329	2,8500	2,4130	1,9309	1,4020	0,9436	0,6614	0,4306
2880	2,9955	2,9096	2,4620	1,9731	1,4306	0,9678	0,6742	0,4411
2910	3,0570	2,9697	2,5129	2,0123	1,4598	0,9870	0,6885	0,4493
2940	3,1193	3,0324	2,5629	2,0530	1,4900	1,0050	0,6991	0,4567
2970	3,1848	3,0947	2,6146	2,0933	1,5218	1,0226	0,7146	0,4646
3000	3,2501	3,1581	2,6666	2,1351	1,5492	1,0422	0,7256	0,4735
3030	3,3143	3,2219	2,7194	2,1774	1,5811	1,0615	0,7401	0,4809
3060	3,3772	3,2856	2,7719	2,2195	1,6069	1,0835	0,7544	0,4877
3090	3,4455	3,3508	2,8244	2,2620	1,6411	1,1062	0,7672	0,4952
3120	3,5127	3,4150	2,8803	2,3038	1,6701	1,1246	0,7811	
3150	3,5792	3,4802	2,9359	2,3481	1,7006			
3180	3,6467	3,5462	2,9890					